

Atomic Transition Probabilities for Forbidden Lines of the Iron Group Elements: (A Critical Data Compilation for Selected Lines)

Cite as: Journal of Physical and Chemical Reference Data **2**, 85 (1973); <https://doi.org/10.1063/1.3253113>
Published Online: 29 October 2009

M. W. Smith, and W. L. Wiese



[View Online](#)



[Export Citation](#)

ARTICLES YOU MAY BE INTERESTED IN

[Atomic transition probabilities for iron, cobalt, and nickel \(A critical data compilation of allowed lines\)](#)

Journal of Physical and Chemical Reference Data **10**, 305 (1981); <https://doi.org/10.1063/1.555644>

[Atomic transition probabilities for scandium and titanium \(A critical data compilation of allowed lines\)](#)

Journal of Physical and Chemical Reference Data **4**, 263 (1975); <https://doi.org/10.1063/1.555519>

[Handbook of Basic Atomic Spectroscopic Data](#)

Journal of Physical and Chemical Reference Data **34**, 1559 (2005); <https://doi.org/10.1063/1.1800011>

Where in the world is AIP Publishing?
Find out where we are exhibiting next



Atomic Transition Probabilities for Forbidden Lines of the Iron Group Elements

(A Critical Data Compilation for Selected Lines.)

M. W. Smith[†] and W. L. Wiese

Institute for Basic Standards, National Bureau of Standards, Washington, D.C., 20234

Atomic transition probabilities for about 750 forbidden spectral lines for elements of the iron group, specifically V, Cr, Mn, Fe, Co, and Ni, have been critically evaluated and compiled using all available literature sources. The selection of the spectra and elements has been made primarily according to their astrophysical importance. The data are presented in separate tables for each element and stage of ionization, and for each ion the data are arranged according to multiplets. For each line within a multiplet the transition probability for spontaneous emission is listed along with the standard spectroscopic designation, the wavelength, the statistical weights, and the energy levels of the upper and lower states. In addition, the estimated accuracy and the source are indicated. In short introductions which precede the individual tables for the ions the main justifications for the choice of the adopted data and for the accuracy rating are discussed. A general introduction contains a detailed discussion of the critical factors entering into the calculations. It also includes detailed comparisons of calculated data with astrophysical observations and a few laboratory results, which serve as a valuable indication for the validity of the estimated accuracies.

Key words: Chromium; cobalt; forbidden transitions; iron; manganese; nickel; transition probabilities; vanadium.

Contents

	Page		Page
A. General Introduction.....	85	Fe IV.....	108
B. List of Abbreviations and Units Used in the Tables.....	91	Fe V.....	109
C. Tabular Material.....	93	Fe VI.....	110
 List of Tables		Fe VII.....	111
 Spectrum		Fe VIII.....	112
Vanadium V x.....	93	Fe IX.....	112
Chromium Cr II.....	93	Fe X.....	113
Cr IX.....	93	Fe XI.....	113
Cr XI.....	93	Fe XII.....	113
Cr XII.....	93	Fe XIII.....	113
Manganese Mn I.....	94	Fe XIV.....	113
Mn V.....	94	Fe XV.....	113
Mn VI.....	95	Cobalt Co XII.....	114
Mn XII.....	95	Nickel Ni I.....	114
Mn XIII.....	96	Ni II.....	116
Iron Fe I.....	96	Ni III.....	118
Fe II.....	99	Ni IV.....	119
Fe III.....	107	Ni XII.....	120
		Ni XIII.....	120
		Ni XV.....	120
		Ni XVI.....	120

A. General Introduction

1. Introductory Remarks

In the following, we present a compilation of atomic transition probabilities for prominent forbidden lines in the spectra of the iron group elements. As in our two

previous critical compilations [1, 2], we include as forbidden lines all magnetic dipole, magnetic quadrupole, and electric quadrupole transitions; that is, all transitions which do not fulfill the rigorous selection rules for electric dipole lines. All material on forbidden lines in the iron group elements comes from calculations; no direct experimental data are available as yet. The principal sources have been the very extensive calculations by Garstang [3, 4, 5, 6, 7, 8] and by Nussbaumer, Swings, and co-workers [9, 10, 11, 12] for transitions within and between configurations of the types $3d^n$, $3d^{n-1}4s$,

[†]Deceased.

Copyright © 1973 by the U.S. Secretary of Commerce on behalf of the United States. This copyright will be assigned to the American Institute of Physics and the American Chemical Society, to whom all requests regarding reproduction should be addressed.

and $3d^{n-2}4s^2$. For the very highly ionized ions, usually representing transitions within various $3p^n$ configurations, we have made use of the works of Krueger and Czyzak [13, 14], Naqvi [15], Malville and Berger [16], and Garstang [17, 18].

2. Scope of This Compilation

We have limited our tabulations to the stronger lines in the optical and near optical region of each spectrum. A number of these forbidden lines have been observed in low density astrophysical objects (e.g., the solar corona, nebulae, etc.) where collisional de-excitation is slower than radiative de-excitation. Discussing first the lower stages of ionization, we have usually selected for inclusion in the tables about $\frac{1}{4}$ to $\frac{1}{2}$ of all those lines for which calculations exist (e.g., see Garstang's papers [4, 5, 6] for Fe II-V). In general, the listed lines account for approximately 95 percent of the intensities within the individual multiplets and also for about 95 percent of the radiative de-excitation processes from a given excited atomic level. These two conditions sometimes necessitate including lines whose wavelengths are in

the infrared. However, in most cases the transition probabilities of these lines are quite small due to the small frequency factor and, therefore, are not tabulated. Other lines for which calculations exist are not tabulated if they involve states whose energy levels must either be calculated or are so highly excited that these states are not likely to be significantly populated. For the higher stages of ionization after the $3d$ and $4s$ electrons are stripped off, the spectra are less complex since only the $3p$ shell is involved. For these spectra we have attempted to present data for all those lines which are observed.

We have also been quite selective in the choice of the listed spectra. While theoretical data are available for many of the neutral and multiply-ionized spectra of the fourth-row elements, we have emphasized the higher spectra of iron because of their obvious astrophysical importance. We have also included, for the same reason, various multiply-ionized spectra of nickel and a few ions of vanadium, chromium, manganese, and cobalt. For many of the remaining ions, no wavelengths have been observed as yet; consequently, no transition probabilities are presented here. Table 1 gives a survey of the

TABLE 1. Availability of transition probabilities for forbidden lines of the iron group. Listed for each spectrum is the complete literature by reference numbers. We have underlined those references which are used for this compilation.

	Sc	Ti	V	Cr	Mn	Fe	Co	Ni
I.....	—	—	—	26	10	11, 28	—	3
II.....	19	23	—	3, <u>9</u>	—	4, 12, 23, 29	40	7
III.....	—	3, 19	23	—	—	5	23	7
IV.....	—	—	19	3, 23, 24	—	6	—	8, 23
V.....	15, 20, 21	—	—	19	3, <u>24</u>	5	—	—
VI.....	15, 16	15, 20, 21	—	—	3, 19	3, 24	—	—
VII.....	—	15, 16, 24	15, 20	27	—	3, <u>19</u> , 24	—	—
VIII.....	15, 16	—	15, 16, 24	15, 20	27	30	19	—
IX.....	15, 20, 22	15, 16	—	13, 15, 16, 24	15, 20	17, 27, <u>31</u>	—	19
X.....	15, 21	15, 20	13, 15, 16, 25	—	13, 15, 16, 24	14, 15, 20, 32, 33	27	—
XI.....	—	15	15, 20	13, 15, 16, 25	—	13, 14, 15, 16, 24, 32, 33	15, 20	27, 31
XII.....	—	—	15	15, <u>20</u>	13, 15, 16, 25	14, 18	13, 15, 16, 25	13, 15, 20, 32, 33
XIII.....	20	—	—	15	13, 15, 20, 25	13, 14, 15, 16, 32, 33, 34	—	15, 16, 32, 33
XIV.....	—	20	—	—	15	14, 15, 20, 32, 33, 35, 36	15, 16	—
XV.....	—	—	20	—	—	14, 15, 17, 32, 37, 38	13, 15, 20, 25	13, 15, 16, 32, 33
XVI.....	16	—	—	20	—	14, 36, 61	13, 15	13, 15, 20, 32, 33
XVII.....	20	16	—	—	20	17	61	13
XVIII.....	—	20	—	—	—	20	—	61
XIX.....	—	—	—	—	—	—	—	—
XX.....	—	—	—	—	—	—	—	—
XXI.....	—	—	—	—	—	39	—	—
XXII.....	—	—	—	—	—	—	—	—
XXIII.....	—	—	—	—	—	17	—	—
XXIV.....	—	—	—	—	—	—	—	—
XXV.....	—	—	—	—	—	17	—	—

availability of calculations of transition probabilities for spectra which we have not tabulated and indicates the references from which these data may be obtained.

A major problem in a compilation of this type is the scarcity of observed wavelengths for the higher stages of

ionization of these elements. The lines are usually seen only in astrophysical objects and many discrepancies exist in the identifications within a spectrum and even in the assignment of the element or stage of ionization. We therefore undertook a rather extensive search of the

recent relevant literature to be able to make judgments of the most reliable wavelengths. The reference sources for these wavelengths are summarized in table 2. It

TABLE 2. List of literature sources used for spectral line identifications and wavelength data. If energy level data other than from the standard energy level tables [ref. 45] are used, the references are listed here, too. The listing of ref. [45] in this table indicates that, for this spectrum, the energy level data have been employed to calculate wavelengths.

Spectrum	Reference No.	Spectrum	Reference No.
V X.....	41	IX.....	17,31
Cr II.....	9	X.....	41
IX.....	41,56	XI.....	41,49,50
XI.....	41,42	XII.....	49,50
XII.....	41	XIII.....	41,49,50
Mn I.....	10	XIV.....	41
V.....	43,44	XV.....	41,51
VI.....	43,44	Co XII.....	41,52
XII.....	41	Ni I.....	44,45
XIII.....	41	III.....	44,45,46
Fe I.....	11,44,45	III.....	53
II.....	44,45,46	IV.....	54
III.....	43,44,47	XII.....	41,55
IV.....	48	XIII.....	41,49,55,56
V.....	43,44,47	XV.....	41,49,55
VI.....	43,44	XVI.....	41,55
VII.....	43,44,45		

should be emphasized that many of the wavelengths for the higher stages of ionization are at this time very uncertain due to the lack of sufficient observational material. Also, it must be noted that all of the wavelength data for forbidden transitions, which we have taken from the Revised Multiplet Table [44], are calculated from energy level differences. We have marked with square brackets those energy levels which are obtained as eigenvalues of wave function calculations, since these are relatively uncertain compared to the other data. We have also used square brackets for ionization potential values, which are obtained either from approximate calculations or extrapolations [77].

3. Outline of the Calculations

We discuss in the following only calculations for the lower stages of ionization of the iron group elements, i.e., those spectra involving transitions within and between configurations of the type $3d^n$, $3d^{n-1}4s$, and $3d^{n-2}4s^2$. For the highly ionized spectra involving transitions within the various $3p^n$ configurations, we refer to the detailed discussion which we have given in ref. [2].

Garstang [3, 4, 5, 6, 7, 8] has repeatedly discussed the method of calculation in detail. The following outline summarizes his explanations: The first step in the calculation of forbidden line strengths is the setting up of the line strength matrices in *LS* coupling. The explicit formulae for magnetic dipole strengths in *LS* coupling, as derived by Shortley [57], are employed; while for electric quadrupole lines, first Pasternack [24] and then

Garstang [58, 59], have derived analogous, more complex formulae.

The second step in the calculations is the determination of the energy matrices for the electrostatic and spin-orbit interactions. Configuration interaction is also considered; however, because of the additional complexities introduced, this effect is normally included only when the interacting configurations are not well separated.

The third step is the choice of numerical values for the parameters (which are various combinations of the Slater integrals, the spin-orbit term ζ_a , and an α term from the $\alpha L(L+1)$ correction) occurring in the energy matrices. Normally these parameters are chosen so as to obtain the best possible agreement between the eigenvalues of the matrices and experimental spectroscopic energy levels. For some highly ionized spectra this is not possible since no observational material is available as yet; the parameters are then obtained entirely from theory.

In the fourth step, the radial integral s_q must be determined for the electric quadrupole line strengths. The evaluation of this integral requires the calculation of the radial wave functions which are usually obtained by means of the well-known self-consistent field method.

4. Assessment of Accuracies

It has been repeatedly pointed out in the literature that it is virtually impossible to make a precise estimate of the accuracy of calculations of this nature. The only way of obtaining some idea of the reliability of the theoretical data is by comparison with experimental material. A few direct comparisons with measurements for simpler atoms are available and have been listed in the introduction of ref. [2]. These selected comparisons are repeated (and updated) here in table 3 so that one may obtain some idea of the accuracy which may be expected. The comparisons indicate that the calculations of prominent forbidden lines of simpler atomic systems are reliable to within 50 percent or better. The highly ionized spectra of the iron group elements, which involve transitions within the various $3p^n$ configurations (i.e., the $3d$ and $4s$ electrons are stripped off) may be considered as such simple atomic systems. It is thus sensible to continue for these spectra with the error classification scheme devised for our previous compilations [1, 2]. In this scheme we have set up ranges of uncertainty differing by about a factor of two and have assigned each transition to such an uncertainty class. We use again the previously applied notation, but need only the following three classifications:

- B.....for uncertainties within 10%,
- C.....for uncertainties within 25%,
- D.....for uncertainties within 50%.

In addition, we occasionally use the classification

DE.....for uncertainties within a factor of two.

TABLE 3. Comparisons of calculated and measured transition probability data for forbidden lines

Element and transition(s)	Experiment				Theory				
	Hertel and Ross [62]	Derwent and Thrush [63]	McConkey and Kernahan [64]	Corney and Williams [65]	Ali [66]	Garstang [3]	O'Brien and Bowen [67]	Garstang [68]	Nicolaides, Sinanoglu, and Westhaus [69]
[Na I]: $3s^2S - 3d^2D$	690 ± 69	—	—	—	612	—	—	—	—
[I I]: $5p^5 {}^2P_{3/2}^o - 5p^5 {}^2P_{1/2}^o$	—	5.9 ± 1.4	—	—	—	7.8	9.1	—	—
[O I]*: Sum of ${}^1D_2 - {}^1S_0$ and ${}^3P_1 - {}^1S_0$	—	—	1.07^*	1.31 ± 0.05	—	—	—	1.35^*	1.25^*

b. Transition probability ratios for some forbidden lines of O I and S I

Element and wavelength	Experiment				Theory
	LeBlanc et al. [71]	McConkey et al. [72]	Kvifte and Vegard [73]	Liszka and Niewodniczanski [74]	Garstang [68]
O I:					
5577/2972	22 ± 2	18.6	—	—	17.6
6363/6300	—	0.33	0.33	—	0.32
2972/2958	—	> 200	—	45	210
S I: 7725/4589		McConkey et al. [75]			Czyzak and Krueger [76]
		5.1 ± 0.7			5.09

*We present in this case the transition probability sum from the $2p^4 {}^1S_0$ state in order to include the accurate lifetime data of Corney and Williams [65] in this comparison. For this purpose we have added to all other data the (small) contribution of the transition probability for the

$2p^4 {}^3P_1 - 2p^4 {}^1S_0$ transition ($A = 0.07 \text{ s}^{-1}$), taken from Yamanouchi and Horie [70]. The other contributions are negligible.

TABLE 4. Comparisons of calculated transition probabilities ($g_k A_{ki}$) with astrophysically observed intensities for [Fe II]. The listed data are normalized independently within each multiplet. The astrophysical observations are usually eye-estimates.

Multiplet (No.)	$\lambda(\text{\AA})$	Theory		Astrophysical observations		
		Garstang [4]		Thackeray [46]	Fehrenbach [60]	Nussbaumer & Swings [10]
		m.d.	e.q.			
$a^6D - b^4P$ (4F)	4889.6	1		1	1	—
	4728.1	0.89		1	1.4	—
	4639.7	0.45		0.8	0.7	—
	4798.2	0.15		0.25	—	—
	4664.4	0.14		0.3	0.5	—
$a^6D - b^4F$ (6F)	4458.0	1		1	1	—
	4382.8	0.19		0.2	0.2	—
	4432.4	0.14		0.2	—	—
	4528.4	0.12		0.2	—	—
	4416.3	2.0		—	2.0	—
	4492.6	0.26		—	0.3	—
$a^6D - a^6S$ (7F)	4287.4		3.0	—	3.6	5
	4359.3		2.2	—	2.1	3
	4413.8		1.6	—	2.0	2.5
	4452.1		1	1	1	1
	4474.9		0.50	0.6	0.3	—
$a^4F - a^2G$ (14F)	7155.1	1		1	—	—
	7452.5	0.32		0.6	—	—
	7172.0	0.30		0.2	—	—
	7388.2	0.23		0.45	—	—
$a^4F - a^2D$ (17F)	5527.3	1		1	—	—
	5412.6	0.67		0.5	—	—
	5495.8	0.35		0.3	—	—
$a^4F - a^4H$ (19F)	5261.6		1	1	—	—
	5333.6		0.70	0.8	—	—
	5376.5		0.57	1	—	—
	5111.6		0.32	0.4	—	—
	5220.1		0.30	0.3	—	—
	5296.8		0.20	0.3	—	—
	5072.4		0.06	0.07	—	—
	5184.8		0.05	0.07	—	—
$a^4F - b^4F$ (20F)	4814.6	1	1	1	—	—
	4905.3	0.45	0.6	0.3	—	—
	4774.7	0.26	0.4	0.3	—	—
	4874.5	0.26	0.4	0.3	—	—
	4973.4	0.21	0.4	—	—	—
	4950.7	0.17	0.4	—	—	—
	4947.4	0.13	0.3	—	—	—
	4852.7	0.02	0.08	—	—	—
$a^4F - a^4G$ (21F)	4244.0	1.7	—	1.5	3	—
	4276.8	1	1	1	1	—
	4358.4	0.68	—	0.7	0.8	—
	4319.6	0.65	0.8	0.7	1	—
	4352.8	0.48	—	0.4	0.8	—
	4346.8	0.38	—	0.5	—	—
	4372.4	0.34	0.45	0.3	—	—
	4244.8	0.31	—	0.4	—	—
	4305.9	0.29	0.4	0.2	—	—
	4177.2	0.22	0.5	0.5	—	—

Turning now to the more complex atomic systems representing the lower ions and neutral atoms in the iron group, it does not seem to be justified to draw any conclusions or make extrapolations from the above discussed comparisons for the simpler atoms. Fortunately, a few somewhat indirect comparisons with observational data for [Fe II], [Fe III], and [Ni II] are available from astrophysical spectra of nebulae, etc. Very extensive comparisons of calculated values within multiplets with observational intensities of [Fe II] and [Ni II] lines from η Carinae have been made by Thackeray [46]. Other recent comparisons with astrophysical intensity measurements for [Fe II] have been carried out by Nussbaumer and Swings [10] and by Fehrenbach [60]. We reproduce in table 4 a representative selection consisting of several multiplets from these comparisons. Some additional comparisons of the same kind have also been undertaken by Garstang for [Fe III] [5]. All these comparisons indicate that within the multiplets the agreement with the calculations is remarkably good. We therefore estimate roughly that the theoretical data should be reliable to within a factor of two for the prominent forbidden lines, with the strongest lines expected to be slightly more accurate than those of only moderate strength. More precise estimates of the accuracy of these forbidden transition probabilities for the lower ions of the iron group—for example, a more detailed error classification as used for the simpler atomic systems—must wait until more detailed and accurate comparisons with laboratory data are available.

Acknowledgments

We would like to express our sincere thanks to Dr. R. H. Garstang for many helpful discussions.

References

- [1] Wiese, W. L., Smith, M. W., and Glennon, B. M., Atomic Transition Probabilities—Hydrogen through Neon (A Critical Data Compilation), Nat. Stand. Ref. Data Ser., Nat. Bur. Stand. (U.S.), **4**, Vol. 1, U.S. Government Printing Office, Washington, D.C. 20402 (May 1966).
- [2] Wiese, W. L., Smith, M. W., and Miles, B. M., Atomic Transition Probabilities—Sodium through Calcium (A Critical Data Compilation), Nat. Stand. Ref. Data Ser., Nat. Bur. Stand. (U.S.), **22**, Vol. 2, U.S. Government Printing Office, Washington, D.C. 20402 (Oct. 1969).
- [3] Garstang, R. H., J. Res. Nat. Bur. Stand., Sect. A, **68**, 61 (1964).
- [4] Garstang, R. H., Mon. Notic. Roy. Astron. Soc. **124**, 321 (1962).
- [5] Garstang, R. H., Mon. Notic. Roy. Astron. Soc. **117**, 393 (1957).
- [6] Garstang, R. H., Mon. Notic. Roy. Astron. Soc. **118**, 572 (1958).
- [7] Garstang, R. H., Mon. Notic. Roy. Astron. Soc. **118**, 234 (1958).
- [8] Garstang, R. H., Astrophys. Space Sci. **2**, 336 (1968).
- [9] Nussbaumer, H., and Swings, J. P., Astrophys. J. **162**, 589 (1970).
- [10] Nussbaumer, H., and Swings, J. P., Astrophys. J. **172**, 121 (1972).
- [11] Grevesse, N., Nussbaumer, H., and Swings, J. P., Mon. Notic. Roy. Astron. Soc. **151**, 239 (1971).
- [12] Nussbaumer, H., and Swings, J. P., Astron. Astrophys. **7**, 455 (1970).
- [13] Krueger, T. K., and Czyzak, S. J., Astrophys. J. **144**, 1194 (1966); **149**, 237 (1967).
- [14] Krueger, T. K., and Czyzak, S. J., Mem. Roy. Astron. Soc. **69**, 145 (1965).
- [15] Naqvi, A. M., Thesis, Harvard (1951).
- [16] Malville, J. M., and Berger, R. A., Planet. Space Sci. **13**, 1131 (1965).
- [17] Garstang, R. H., Publ. Astron. Soc. Pac. **81**, 488 (1969).
- [18] Garstang, R. H., to be published (1972).
- [19] Warner, B., and Kirkpatrick, R. C., Mon. Notic. Roy. Astron. Soc. **144**, 397 (1969).
- [20] Warner, B., Z. Astrophys. **69**, 399 (1968).
- [21] Mizushima, M., J. Phys. Soc. Jap. **21**, 2335 (1966).
- [22] Nikitin, A. A., and Yakubovskii, O. A., Sov. Phys.—Dokl. **9**, 409 (1964).
- [23] Rudzikas, Z. B., and Yutsis, A. P., Litov. Fiz. Sb. **9**, 433 (1969).
- [24] Pasternack, S., Astrophys. J. **92**, 129 (1940).
- [25] Pottasch, S. R., Mon. Notic. Roy. Astron. Soc. **128**, 73 (1964).
- [26] Synék, M., and Lichodziejewski, W., Phys. Lett. **22**, 578 (1966).
- [27] Wagner, W. J., and House, L. L., Astrophys. J. **155**, 677 (1969).
- [28] Grevesse, N., and Swings, J. P., Astron. Astrophys. **2**, 28 (1969).
- [29] Mel'nikov, O. A., Sov. Astron.—AJ **3**, 381 (1959).
- [30] Czyzak, S. J., and Krueger, T. K., Astrophys. J. **144**, 381 (1966).
- [31] Wagner, W. J., and House, L. L., Astrophys. J. **166**, 683 (1971).
- [32] Edlén, B., Z. Astrophys. **22**, 30 (1942).
- [33] Huang, K., Astrophys. J. **101**, 187 (1945).
- [34] Kurt, V. G., Sov. Astron.—AJ **6**, 620 (1963).
- [35] Garstang, R. H., Ann. Astrophys. **25**, 109 (1962).
- [36] Steele, R., and Trefftz, E., J. Quant. Spectrosc. Radiat. Transfer **6**, 833 (1966).
- [37] Osterbrock, D. E., Astrophys. J. **114**, 469 (1951).
- [38] Blaha, M., Central Astronomical Institutes of Czechoslovakia: Bulletin **8**, 34 (1957).
- [39] Nussbaumer, H., Astrophys. J. **166**, 411 (1971).
- [40] Kychkin, I. S., Rudzikas, Z. B., and Vizbaraité, Ya. I., Litov. Fiz. Sb. **10**, 47 (1970).
- [41] Jefferies, J. T., Mem. Soc. Roy. Sci. Liege, Ser. 5, **17**, 213 (1969); Jefferies, J. T., Orrall, F. Q., and Zirker, J. B., Mem. Soc. Roy. Sci. Liege, Ser. 5, **17**, 235 (1969).
- [42] Olsen, K. H., Anderson, C. R., and Stewart, J. N., Solar Phys. **21**, 360 (1971).
- [43] Bowen, I. S., Astrophys. J. **121**, 306 (1955).
- [44] Moore, C. E., A Multiplet Table of Astrophysical Interest, Revised Edition, Nat. Bur. Stand. (U.S.), Tech. Note 36, U.S. Government Printing Office, Washington, D.C. 20402 (Nov. 1959).
- [45] Moore, C. E., Atomic Energy Levels, Nat. Bur. Stand. (U.S.), Circ. 467, Vol. II, U.S. Government Printing Office, Washington, D.C. 20402 (Aug. 1952).
- [46] Thackeray, A. D., Mon. Notic. Roy. Astron. Soc. **135**, 51 (1967).
- [47] Bowen, I. S., Astrophys. J. **132**, 1 (1960).
- [48] Edlén, B., Mon. Notic. Roy. Astron. Soc. **144**, 391 (1969).
- [49] Jordan, C., Solar Phys. **21**, 381 (1971).
- [50] Fawcett, B. C., J. Phys. B, **4**, 1577 (1971).
- [51] Bely, O., and Blaha, M., Solar Phys. **3**, 563 (1968).
- [52] Nikol'skii, G. M., Sov. Astron.—AJ **10**, 915 (1967).
- [53] Shenstone, A. G., J. Opt. Soc. Amer. **44**, 749 (1954).
- [54] Lambert, D. L., and Thackeray, A. D., Astrophys. Space Sci. **5**, 283 (1969).
- [55] Fawcett, B. C., and Hayes, R. W., J. Phys. B, **5**, 366 (1972).
- [56] Jefferies, J. T., Orrall, F. Q., and Zirker, J. B., Solar Phys. **22**, 317 (1972).
- [57] Shortley, G. H., Phys. Rev. **57**, 225 (1940).
- [58] Garstang, R. H., Proc. Cambridge Phil. Soc. **53**, 214 (1957).
- [59] Garstang, R. H., Proc. Cambridge Phil. Soc. **54**, 383 (1958).
- [60] Fehrenbach, C., Astron. Astrophys. **13**, 437 (1971).
- [61] Tull, C. E., Jackson, M., McEachran, R. P., and Cohen, M. J., Quant. Spectrosc. Radiat. Transfer **12**, 893 (1972).
- [62] Hertel, I. V., and Ross, K. J., J. Phys. B **2**, 285 (1969).

- [63] Derwent, R. G., and Thrush, B. A., Chem. Phys. Lett. **9**, 591 (1971).
- [64] McConkey, J. W., and Kernahan, J. A., Planet. Space Sci. **17**, 1297 (1969).
- [65] Corney, A., and Williams, O. M., J. Phys. B **5**, 686 (1972).
- [66] Ali, M. A., J. Quant. Spectrosc. Radiat. Transfer **11**, 1611 (1971).
- [67] O'Brien, D. E., and Bowen, J. R., J. Appl. Phys. **40**, 4767 (1969).
- [68] Garstang, R. H., Mon. Notic. Roy. Astron. Soc. **111**, 115 (1951).
- [69] Nicolaides, C., Sinanoglu, O., and Westhaus, P., Phys. Rev. A **4**, 1400 (1971).
- [70] Yamanouchi, T., and Horie, H., J. Phys. Soc. Jap. **7**, 52 (1952).
- [71] LeBlanc, F. J., Oldenberg, O., and Carleton, N. P., J. Chem. Phys. **45**, 2200 (1966).
- [72] McConkey, J. W., Burns, D. J., Moran, K. A., and Emeleus, K. G., Phys. Lett. **22**, 416 (1966).
- [73] Kvifte, G., and Vegard, L., Geofys. Publ. **17**, No. 1 (1947).
- [74] Liszka, L., and Niewodniczanski, H., Acta Phys. Pol. **17**, 345 (1958).
- [75] McConkey, J. W., Burns, D. J., Moran, K. A., and Kernahan, J. A., Nature (London) **217**, 538 (1968).
- [76] Czyzak, S. J., and Krueger, T. K., Mon. Notic. Roy. Astron. Soc. **126**, 177 (1963).
- [77] Moore, C. E., Ionization Potentials and Ionization Limits Derived from the Analysis of Optical Spectra, Nat. Stand. Ref. Data Ser., Nat. Bur. Stand. (U.S.) **34**, U.S. Government Printing Office, Washington, D.C. 20402 (Sept. 1970).

B. List of Abbreviations and Units Used in the Tables

1. Types of forbidden lines:

e=electric quadrupole,
m=magnetic dipole,
mq=magnetic quadrupole.

The total transition probability is obtained by adding the individual transition probabilities due to each type of radiation. It is assumed that there are no significant

magnetic fields present, i.e., the transition probabilities represent the usual average over the magnetic sublevels.

2. The numbers in the lists of tabulated lines refer to the running multiplet numbers of the tables. ("Lists of tabulated lines" have been given for all spectra where 20 or more lines have been tabulated).

3. The number in parenthesis under the multiplet notation refers to the running number of the "Revised Multiplet Table" (ref. [44]).

4. Energy levels and ionization potentials appearing in square brackets indicate approximately calculated or extrapolated values.

5. The statistical weight g_L for level L is given by

$$g_L = 2J_L + 1,$$

where J_L is the inner or total angular momentum quantum number.

6. Letters used for the indication of accuracy:

- B..... uncertainties within 10%,
- C..... uncertainties within 25%,
- D..... uncertainties within 50%,
- DE..... uncertainties within a factor of 2.

7. Other abbreviations:

n.....(in the "Source" column) indicates that data have been renormalized as described in the introduction to that spectrum.

C. Tabular Material

Vanadium

[V x]

Ground State $1s^2 2s^2 2p^6 3s^2 3p^2 3P$

Ionization Potential $[1859200] \text{cm}^{-1} = [230.5] \text{eV}$

For this spectrum, calculations by Krueger and

Czyzak [13] are available and have been used for this tabulation. These calculations are based on self-consistent field wave functions and include the spin-orbit and spin-spin and spin-other-orbit interactions; experimental values for the energy intervals are used whenever available.

[V x]

No.	Transition array	Multiplet	$\lambda(\text{\AA})$	$E_i(\text{cm}^{-1})$	$E_k(\text{cm}^{-1})$	g_i	g_k	Type of transition	$A_{ki}(\text{s}^{-1})$	Accuracy	Source
1.	$3p^2-3p^2$	$3P-1D$	4312	—	—	5	5	m	16.3	C	13
			3534	—	—	3	5	m	10.2	C	13

Chromium

[Cr II]

Ground State $1s^2 2s^2 2p^6 3s^2 3p^6 3d^5 6S_{5/2}$

Ionization Potential $133060 \text{ cm}^{-1} = 16.50 \text{ eV}$

The values for the one multiplet listed for this ion are taken from the calculations of Nussbaumer and Swings

[9]. This calculation includes the spin-orbit interaction but does not include the effects of configuration interaction in the quadrupole moment s_q ; however, from comparisons with Garstang's previous work [3], the authors estimate that their results should be reliable to better than a factor of 2.

[Cr II]

No.	Multiplet	$\lambda(\text{\AA})$	$E_i(\text{cm}^{-1})$	$E_k(\text{cm}^{-1})$	g_i	g_k	Type of transition	$A_{ki}(\text{s}^{-1})$
1.	a^6S-a^6D (1F)	7999.85	0	12497	6	10	e	0.10
		8125.22	0	12304	6	8	e	0.094
		8229.55	0	12148	6	6	e	0.088
		8308.39	0	12033	6	4	e	0.084
		8357.51	0	11962	6	2	e	0.082

[Cr IX]-[Cr XII]

Ion	Ground state	Ionization potential
[Cr IX]	$1s^2 2s^2 2p^6 3s^2 3p^4 3P_2$	$[1688000] \text{ cm}^{-1} = [209.3] \text{eV}$
[Cr XI]	$1s^2 2s^2 2p^6 3s^2 3p^2 3P_0$	$[2184000] \text{ cm}^{-1} = [270.8] \text{eV}$
[Cr XII]	$1s^2 2s^2 2p^6 3s^2 3p^2 P_{1/2}^o$	$[2403600] \text{ cm}^{-1} = [298.0] \text{eV}$

(a) For the spectrum of [Cr IX], calculations by Krueger and Czyzak [13] are available and have been

used for this tabulation. These calculations are based on self-consistent field wave functions and include the spin-orbit and spin-spin and spin-other-orbit interactions; experimental values for the energy intervals are used whenever available. From a study of the recent literature it appears that the wavelength identifications for this ion are particularly uncertain [41, 56].

(b) Since no wavelengths have as yet been observed for [Cr X] and no calculations of forbidden transition probabilities exist, we can not present any data.

(c) For the spectrum of [Cr XI], calculations by Krueger and Czyzak [13] are available and have been used for this tabulation. These calculations are based on self-consistent field wave functions and include the spin-orbit and spin-spin and spin-other-orbit interactions; experimental values for the energy intervals are used whenever available.

(d) For [Cr XII], the line strength for the one magnetic dipole transition in the ground state configuration is

a straight number which has been, for example, tabulated by Naqvi [15] or Warner [20] (listed also in the General Introduction of our previous transition probability compilation, NSRDS-NBS 22, table 4 [2]). The quantity presented here, the transition probability, should also be quite accurate, since the energy level difference required for the conversion from the line strength is accurately known from the line observed in the solar corona.

[Cr IX]–[Cr XII]

Ion	No.	Transition array	Multiplet	$\lambda(\text{\AA})$	$E_i(\text{cm}^{-1})$	$E_k(\text{cm}^{-1})$	g_i	g_k	Type of transition	$A_{ki}(\text{s}^{-1})$	Accuracy	Source
[Cr IX]	1.	$3p^4-3p^4$	$^3P-^1D$ (1F)	3303	0	30270	5	5	<i>m</i>	30.7	C	13
				4452	7860	30270	3	5	<i>m</i>	4.31	C	13
[Cr XI]	1.	$3p^2-3p^2$	$^3P-^3P$	15230	5389	11954	3	5	<i>m</i>	3.60	C	13
				18560	0	5389	1	3	<i>m</i>	2.72	C	13
[Cr XII]	2.	$3p-3p$	$^3P-^1D$	3997	11954	36961	5	5	<i>m</i>	28.6	C	13
				8154	0	12261	2	4	<i>m</i>	16.6	B	2, 15, 20

Manganese

[Mn I]

Ground State $1s^2 2s^2 2p^6 3s^2 3p^6 3d^5 4s^2 6S_{5/2}$
Ionization Potential $59970 \text{ cm}^{-1} = 7.435 \text{ eV}$

The values for the one multiplet listed for this ion are taken from the calculations of Nussbaumer and Swings

[10]. This calculation includes the spin-orbit interaction and also limited configuration interaction in the quadrupole moment s_q . From comparisons with Garstang's unpublished work (quoted in [10]), the authors estimate that their results should be reliable to better than a factor of 2.

[Mn I]

No.	Multiplet	$\lambda(\text{\AA})$	$E_i(\text{cm}^{-1})$	$E_k(\text{cm}^{-1})$	g_i	g_k	Type of transition	$A_{ki}(\text{s}^{-1})$
1.	a^6S-a^6D	5862.69	0	17052	6	10	<i>e</i>	0.29
		5784.76	0	17282	6	8	<i>e</i>	0.31
		5728.58	0	17452	6	6	<i>e</i>	0.33
		5690.43	0	17568	6	4	<i>e</i>	0.34
		5668.26	0	17637	6	2	<i>e</i>	0.35

[Mn V]

Ground State $1s^2 2s^2 2p^6 3s^2 3p^6 3d^3 4F_{3/2}$
Ionization Potential $[584000] \text{ cm}^{-1} = [72.4] \text{ eV}$

All values for this ion have been taken from Pasterнак [24]. The electric quadrupole values have been

modified by applying Garstang's value [3] for the quadrupole moment s_q which is obtained with better wave functions. Both types of radiation are estimated to be reliable within a factor of 2. The reasons for this estimate are given in the General Introduction.

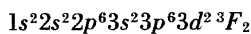
[Mn V]

No.	Multiplet	$\lambda(\text{\AA})$	$E_i(\text{cm}^{-1})$	$E_k(\text{cm}^{-1})$	g_i	g_k	Type of transition	$A_{ki}(\text{s}^{-1})$
1.	a^4F-a^4P (1F)	6393.6	1406	17036	10	6	e	0.041
		6346	827	16580	8	4	e	0.031
		6218.6	349	16420	6	2	e	0.026
		{ 6166.2	827	17036	8	6	m	4.4(-4)* }
		6159	349	16580	6	4	e	0.026
		6088	0	16420	4	2	e	0.044
		{ 5991	349	17036	6	6	m	1.9(-4) }
		6030	0	16580	4	4	m	0.0041 }
							e	5.1(-4) }
							m	0.0093 }
2.	a^4F-a^2G (2F)	5891.1	1406	18382	10	10	m	0.24
		5862.3	827	17878	8	8	m	0.096
		6069	1406	17878	10	8	m	0.0059
		5695	827	18382	8	10	m	0.096
		5703	349	17878	6	8	m	0.088

* The number in parentheses following the tabulated value indicates the power of ten by which this value has to be multiplied.

[Mn VI]

Ground State



Ionization Potential

$$[766000] \text{ cm}^{-1} = [95.0] \text{ eV}$$

of Garstang [3]. His results are estimated to be reliable to within a factor of 2. For a more detailed discussion of the accuracy of transition probabilities for forbidden lines in $3d^n$ configurations and several comparisons with observations, we refer to the General Introduction.

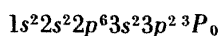
The data for this ion are taken from the calculations

[Mn VI]

No.	Multiplet	$\lambda(\text{\AA})$	$E_i(\text{cm}^{-1})$	$E_k(\text{cm}^{-1})$	g_i	g_k	Type of transition	$A_{ki}(\text{s}^{-1})$	
1.	a^3F-a^1D (1F)	6852	746	15336	7	5	m	0.23	
		6518.3	0	15336	5	5	m	0.14	
		2.	a^3F-a^3P (2F)	1669	18628	9	5	e	0.050
		5776.4	746	18057	7	3	e	0.050	
		5622	0	17782	5	1	e	0.087	
		{ 5591	746	18628	7	5	m	0.013 }	
		5536	0	18057	5	3	e	0.031	
		{ 5367	0	18628	5	5	m	0.0035 }	
							e	0.0028 }	
							m		
3.	a^3F-a^1G (3F)	4193	1669	25511	9	9	m	0.17	
		4037	746	25511	7	9	m	0.12	
4.	a^1D-a^3P	30370	15336	18628	5	5	m	0.060	
		36740	15336	18057	5	3	m	0.020	

[Mn XII]

Ground State



Ionization Potential

$$[2535900] \text{ cm}^{-1} = [314.4] \text{ eV}$$

Calculations by Krueger and Czyzak [13] are available

and have been used for this tabulation. These calculations are based on self-consistent field wave functions and include the spin-orbit and spin-spin and spin-other-orbit interactions; experimental values for the energy intervals are used whenever available.

[Mn XII]

No.	Transition array	Multiplet	$\lambda(\text{\AA})$	$E_i(\text{cm}^{-1})$	$E_k(\text{cm}^{-1})$	g_i	g_k	Type of transition	$A_{ki}(\text{s}^{-1})$	Accuracy	Source
1.	$3p^2-3p^2$	${}^3P-{}^1D$	3686	—	—	5	5	<i>m</i>	48.9	C	13

[Mn XIII]

Ground State $1s^2 2s^2 2p^6 3s^2 3p^2 P_{1/2}^o$
 Ionization Potential $[2771400] \text{ cm}^{-1} = [343.6] \text{ eV}$

The line strength for the one magnetic dipole transition in the ground state configuration is a straight number which has been, for example, tabulated by

Krueger and Czyzak [13] (listed also in the General Introduction of our previous transition probability compilation, NSRDS-NBS 22, table 4 [2]). The quantity presented here, the transition probability, should also be quite accurate, since the energy level difference required for the conversion from the line strength is accurately known from the spectral position of the line observed in the solar corona.

[Mn XIII]

No.	Transition array	Multiplet	$\lambda(\text{\AA})$	$E_i(\text{cm}^{-1})$	$E_k(\text{cm}^{-1})$	g_i	g_k	Type of transition	$A_{ki}(\text{s}^{-1})$	Accuracy	Source
1.	$3p-3p$	$2p^o-2p^o$	6536	0	15298	2	4	<i>m</i>	32.2	B	2, 13

Iron

[Fe I]

Ground State $1s^2 2s^2 2p^6 3s^2 3p^6 3d^6 4s^2 {}^5D_4$
 Ionization Potential $63480 \text{ cm}^{-1} = 7.870 \text{ eV}$

List of tabulated lines

Wavelength [\AA]	No.*						
3403.65	9	5156.32	13	5936.99	2	10056.0	10
3452.54	9	5160.56	4	5968.87	2	10075.0	23
3454.34	9	5220.56	3	5999.99	2	10229.8	10
3487.23	9	5290.75	12	6231.27	18	10235.2	22
3489.07	9	5303.99	3	6393.72	18	10262.8	10
3511.64	9	5304.06	12	6760.61	11	10264.6	14
3516.17	9	5356.32	3	6836.94	11	10315.0	23
3527.33	9	5363.91	12	6884.50	11	10318.7	14
3812.07	8	5382.26	3	6972.07	11	10916.6	24
3856.98	8	5412.97	12	7005.23	11	11202.1	24
3917.64	8	5427.17	12	7008.89	11	11237.0	20
3931.50	8	5439.72	3	7016.21	17	11524.5	20
4153.72	7	5477.40	12	7316.44	17	11764.2	20
4458.57	6	5565.68	3	7321.23	17	12124.5	21
4494.57	6	5639.55	2	7439.58	17	13206.7	1
4510.63	6	5656.39	3	7935.32	16	13417.8	1
4789.19	5	5696.36	2	8321.51	16	13552.3	1
4843.34	5	5708.96	2	9093.67	22	13672.2	1
4847.58	5	5715.94	3	9106.17	22	13729.1	1
4886.56	5	5745.49	3	9203.80	15	13757.8	1
4916.26	5	5775.05	2	9411.90	10	13954.5	19
4942.95	5	5804.45	2	9658.96	10	14072.3	25
4956.35	5	5834.64	2	9801.87	10	14429.7	1
4961.18	5	5867.17	2	9826.83	10	14586.0	21
5052.09	4	5872.77	2	9974.41	14	14657.0	25
5111.78	13	5934.41	2	9998.31	10		

*The numbers in the lists of tabulated lines refer to the running multiplet numbers of the tables. ("Lists of tabulated lines" have been

given for all spectra where 20 or more lines have been tabulated.)

All listed values are taken from the recent calculations of Grevesse et al. [11]. From their more extensive data tables we have presented here the lines of at least moderate strength, which amount to about one-half of those given in their paper. For each line, we have listed only the type of radiation which gives the dominant contribution to A_{ki} ($> 99\%$). Thus, for some lines this required tabulating the magnetic dipole as well as the electric quadrupole contributions when both are nearly

comparable. Grevesse et al. include limited configuration interaction in their calculations, but make no attempt to estimate the accuracy. We estimate, mainly on the basis of our experience with less complex spectra and some comparisons with astrophysical (observed) intensities for similar spectra, that the uncertainties for these relatively prominent lines are within a factor of two. A more detailed discussion of the determination of the uncertainty estimates is given in the General Introduction.

[Fe I]

No.	Multiplet	$\lambda(\text{\AA})$	$E_i(\text{cm}^{-1})$	$E_k(\text{cm}^{-1})$	g_i	g_k	Type of transition	$A_{ki}(\text{s}^{-1})$
1.	a^5D-a^5F	14429.7	0	6928	9	11	e	0.0020
		13552.3	0	7377	9	9	e	0.0015
		13672.2	416	7728	7	7	e	0.0017
		13729.1	704	7986	5	5	e	0.0016
		13757.8	888	8155	3	3	e	0.0019
		13206.7	416	7986	7	5	e	0.0011
		13417.8	704	8155	5	3	e	0.0015
2.	a^5D-a^5P (2F)	5696.36	0	17550	9	7	e	0.12
		5775.05	416	17727	7	5	m	0.0096
		5804.45	704	17927	5	3	e	0.088
		5639.55	0	17727	9	5	e	0.14
		5708.96	416	17927	7	3	e	0.15
		5834.64	416	17550	7	7	e	0.090
		5872.77	704	17727	5	5	e	0.034
		5867.17	888	17927	4	3	e	0.021
		5934.41	704	17550	5	7	e	0.039
		5936.99	888	17727	3	5	e	0.053
		5999.99	888	17550	3	7	e	0.0085
		5968.87	978	17727	1	5	e	0.024
		5439.72	0	18378	9	5	e	0.0053
		5565.68	416	18378	7	5	m	0.36
3.	a^5D-a^3P (3F)	5303.99	704	19552	5	3	m	0.46
		5220.56	888	20038	3	1	m	0.57
		5656.39	704	18378	5	5	e	0.0018
		5356.32	888	19552	3	3	e	0.0010
		{ 5715.94	888	18378	3	5	m	0.034 }
		5382.26	978	19552	1	3	m	0.079
		5745.49	978	18378	1	5	e	0.0020
		5052.09	0	19788	9	9	m	0.0082
		5160.56	416	19788	7	9	m	0.0015
5.	a^5D-b^3F (4F)	4843.34	0	20641	9	9	m	0.42
		4886.56	416	20875	7	7	m	0.23
		4916.26	704	21039	5	5	m	0.092
		4789.19	0	20875	9	7	m	0.039
		4847.58	416	21039	7	5	m	0.025
		4942.95	416	20641	7	9	m	0.077
		4956.35	704	20875	5	7	m	0.079
		4961.18	888	21039	3	5	m	0.045
6.	a^5D-b^3P (6F)	{ 4458.57	416	22838	7	5	m	0.030 }
		{ 4494.57	704	22947	5	3	e	0.003 }
		{ 4510.63	888	23052	3	1	m	0.044 }
		4153.72	704	24772	5	3	m	0.10
7.	a^5D-c^3P (8F)							0.016

[Fe I]—Continued

No.	Multiplet	$\lambda(\text{\AA})$	$E_i(\text{cm}^{-1})$	$E_k(\text{cm}^{-1})$	g_i	g_k	Type of transition	$A_{ki}(\text{s}^{-1})$
8.	a^5D-a^3D (9F)	3812.07	0	26225	9	7	<i>m</i>	0.014
		3856.96	704	26624	5	5	<i>e</i>	0.007
		3917.64	888	26406	3	3	<i>m</i>	0.011
		3931.50	978	26406	1	3	<i>m</i>	0.012
9.	a^5D-b^3D (10F)	3403.65	0	29372	9	7	<i>m</i>	0.18
		3454.34	416	29357	7	5	<i>m</i>	0.021
		3452.54	416	29372	7	7	<i>m</i>	0.052
		3489.07	704	29357	5	5	<i>m</i>	0.083
		3516.17	888	29320	3	3	<i>m</i>	0.10
		3487.23	704	29372	5	7	<i>m</i>	0.037
		3511.64	888	29357	3	5	<i>e</i>	0.002
		3527.33	978	29320	1	3	<i>m</i>	0.070
10.	a^5F-a^5P (11F)	9826.83	7377	17550	9	7	<i>e</i>	0.0029
		9998.31	7728	17727	7	5	<i>e</i>	0.0039
		10056.0	7986	17927	5	3	<i>e</i>	0.0043
		9411.90	6928	17550	11	7	<i>e</i>	0.010
		9658.96	7377	17727	9	5	<i>e</i>	0.0054
		9801.87	7728	17927	7	3	<i>e</i>	0.0029
		10262.8	7986	17727	5	5	<i>e</i>	0.0016
		10229.8	8155	17927	3	3	<i>e</i>	0.0035
		6760.61	6928	21716	11	11	<i>m</i>	0.13
11.	a^5F-a^3G (15F)	6836.94	7377	21999	9	9	<i>m</i>	0.072
		6884.50	7728	22249	7	7	<i>m</i>	0.028
		6972.07	7377	21716	9	11	<i>m</i>	0.026
		7005.23	7728	21999	7	9	<i>m</i>	0.032
		7008.89	7986	22249	5	7	<i>m</i>	0.022
		5304.06	7377	26225	9	7	<i>m</i>	0.18
12.	a^5F-a^3D (20F)	5290.75	7728	26624	7	5	<i>m</i>	0.22
		5427.17	7986	26406	5	3	<i>m</i>	0.17
		5363.91	7986	26624	5	5	<i>m</i>	0.020
		5477.40	8155	26406	3	3	<i>m</i>	0.082
		5412.97	8155	26624	3	5	<i>m</i>	0.022
		5111.78	7986	27543	5	3	<i>m</i>	0.023
13.	a^5F-a^1P	5156.32	8155	27543	3	3	<i>m</i>	0.011
		10264.6	11976	21716	9	11	<i>m</i>	0.011
		9974.41	11976	21999	9	9	<i>m</i>	0.015
14.	a^3F-a^3G (23F)	10318.7	12561	22249	7	7	<i>m</i>	0.012
		9203.80	11976	22838	9	5	<i>e</i>	0.013
		7935.32	11976	24575	9	9	<i>m</i>	0.064
		8321.51	12561	24575	7	9	<i>m</i>	0.041
15.	a^3F-b^3P	7016.21	11976	26225	9	7	<i>m</i>	0.033
		7439.58	12969	26406	5	3	<i>m</i>	0.016
		7316.44	12561	26225	7	7	<i>m</i>	0.020
		7321.23	12969	26624	5	5	<i>m</i>	0.011
16.	a^3F-a^1G (26F)	6231.27	12561	28605	7	5	<i>m</i>	0.17
		6393.72	12969	28605	5	5	<i>m</i>	0.093
		13954.5	17927	25092	3	1	<i>m</i>	0.020
17.	a^3F-a^3D (28F)	11524.5	17550	26225	7	7	<i>m</i>	0.068
		11237.0	17727	26624	5	5	<i>m</i>	0.025
		11764.2	17727	26225	5	7	<i>m</i>	0.015

[Fe I]—Continued

No.	Multiplet	$\lambda(\text{\AA})$	$E_i(\text{cm}^{-1})$	$E_k(\text{cm}^{-1})$	g_i	g_k	Type of transition	$A_{ki}(\text{s}^{-1})$
21.	a^3P-a^3D	12124.5	18378	26624	5	5	<i>m</i>	0.020
		14586.0	19552	26406	3	3	<i>m</i>	0.014
22.	a^3P-b^3D (36F)	{ 9093.67	18378	29372	5	7	<i>m</i>	0.034 }
		{ 9106.17	18378	29357	5	5	<i>e</i>	0.003 }
		{ 10235.2	19552	29320	3	3	<i>m</i>	0.028 }
							<i>e</i>	0.002 }
							<i>m</i>	0.029 }
							<i>e</i>	0.001 }
23.	a^3H-a^1I (38F)	10075.0	19390	29313	13	13	<i>m</i>	0.079
		10315.0	19621	29313	11	13	<i>m</i>	0.052
24.	b^3F-b^1G (41F)	10916.6	20641	29799	9	9	<i>m</i>	0.19
		11202.1	20875	29799	7	9	<i>m</i>	0.092
25.	a^3G-a^1H	14072.3	21716	28820	11	11	<i>m</i>	0.033
		14657.0	21999	28820	9	11	<i>m</i>	0.015

[Fe II]

Ground State

 $1s^2 2s^2 2p^6 3s^2 3p^6 3d^6 4s$ ${}^6D_{9/2}$

Ionization Potential

 $130524 \text{ cm}^{-1} = 16.18 \text{ eV}$

List of tabulated lines

Wavelength [Å]	No.*						
3175.38	5	3505.81	15	4243.98	12	4457.95	3
3214.67	5	3528.28	15	4244.81	12	4468.6	22
3224.54	5	3532.8	25	4251.4	14	4470.29	3
3244.18	5	3536.25	16	4266.34	23	4474.91	4
3254.24	5	3538.69	16	4276.83	12	4479.2	37
3275.02	5	3539.19	16	4280.0	13	4488.75	3
3277.12	5	3575.72	15	4287.40	4	4492.64	3
3277.55	5	3579.81	15	4305.90	12	4509.61	3
3289.46	5	3588.2	25	4319.62	12	4514.90	3
3289.89	5	3604.7	25	4329.43	23	4528.39	3
3318.38	17	3625.7	25	4346.85	12	4533.00	3
3376.20	16	3628.65	15	4351.80	23	4576.2	37
3380.95	17	3642.5	25	4352.78	12	4639.68	2
3387.10	16	3664.8	25	4356.14	13	4664.45	2
3402.50	17	4002.0	29	4358.37	12	4728.07	2
3428.24	17	4083.78	14	4359.34	4	4745.49	11
3440.99	16	4114.48	14	4372.43	12	4772.07	2
3450.39	17	4149.1	13	4382.75	3	4774.74	11
3452.30	16	4157.89	24	4383.0	22	4798.28	2
3455.11	16	4177.21	12	4402.60	23	4814.55	11
3484.01	17	4178.95	14	4409.86	13	4852.73	11
3489.98	16	4197.81	13	4413.78	4	4874.49	11
3501.62	16	4211.1	14	4416.27	3	4889.63	2
3504.02	16	4231.56	12	4432.45	3	4898.7	36
3504.51	16	4234.81	24	4452.11	4	4905.35	11

List of Tabulated Lines—Continued

Wavelength [Å]	No.*						
4947.38	11	5870.0	34	8259.5	45	10796.5	38
4950.74	11	5901.26	20	8305.4	58	10875	64
4973.39	11	5913.1	50	8387.7	58	10888	56
5005.52	11	5982.8	49	8411.7	58	10910	27
5006.65	2	6043.9	34	8480.2	58	10942	27
5020.24	11	6094.8	55	8490.3	31	10955	27
5027.8	36	6188.55	33	8574.7	44	11044	56
5035.4	41	6261.2	33	8575.5	57	11066	27
5043.53	11	6280.1	49	8600.5	57	11159	56
5048.3	41	6353.1	48	8616.96	7	11160	52
5060.1	36	6396.30	33	8708.4	57	11165	38
5072.40	10	6404.8	48	8715.84	31	11351	56
5107.95	9	6473.86	33	8734.3	57	11448	38
5111.63	10	6482.5	53	8739.6	65	11655	60
5158.00	9	6485.4	54	8825.3	57	12569	59
5158.81	10	6511.2	62	8861.3	66	12776	59
5163.94	21	6544.4	62	8885.66	31	12896	59
5172.4	41	6566.3	62	8891.88	7	13191	59
5181.97	9	6584.1	62	8931.47	44	13701	69
5184.80	10	6671.90	19	9033.45	7	13986	69
5186.1	41	6689.4	48	9051.92	7	14053	69
5220.06	10	6700.68	32	9083.5	44	14601	72
5261.61	10	6729.85	19	9133.63	31	14833	68
5268.88	9	6746.7	48	9202.2	61	14908	68
5273.38	9	6747.1	54	9226.60	7	14964	72
5296.84	10	6809.21	19	9231.1	61	15247	68
5333.65	10	6829.01	19	9267.54	7	16161	70
5347.67	9	6872.17	19	9351.1	61	16250	70
5376.47	10	6873.87	32	9380.9	61	16999	70
5433.15	9	6896.18	8	9385.3	52	17148	42
5477.25	20	6922.8	53	9435.8	71	17852	63
5483.90	20	6933.67	19	9465.3	61	18023	42
5527.61	20	6944.91	32	9469.8	52	19522	51
5551.31	28	6966.32	19	9470.93	7	20067	26
5556.31	9	7011.24	19	9491.4	52	20168	51
5580.82	28	7047.99	19	9513.87	30	20457	26
5586.9	28	7131.13	32	9553.1	64	21325	26
5587.5	40	7155.14	8	9590.6	43	22103	51
5588.15	28	7171.98	8	9670.4	64	22436	26
5613.3	28	7330.4	39	9682.13	30	22562	63
5627.5	40	7370.94	18	9711.7	65	22664	67
5649.67	28	7388.16	8	9949.32	43	23696	67
5650.94	28	7432.23	39	10013.9	30	24770	67
5673.2	35	7452.50	8	10038.8	43	25144	51
5718.3	28	7613.15	18	10127	46	29595	51
5725.92	28	7719.9	47	10432.6	43	179330	6
5746.96	20	7734.8	39	10462	52	245120	6
5756.8	40	7764.69	18	10466	52	259820	1
5767.7	55	7974.8	45	10572	46	353420	1
5799.2	40	8044.8	66	10683	27	357630	6
5835.4	35	8077.9	66	10708	27	512710	1
5847.0	35	8199.2	47	10789	27	873890	1

*The numbers in the lists of tabulated lines refer to the running multiplet numbers of the tables. ("Lists of tabulated lines" have been

given for all spectra where 20 or more lines have been tabulated.)

We have exclusively used data from the very extensive calculations by Garstang [4], which include about 1000 lines. A recent calculation by Nussbaumer and Swings [12] confirms, usually within 30 percent, the results of Garstang's magnetic dipole calculations for most of the strong lines. The two calculations disagree, however, by more than a factor of 2 for a few prominent

lines, which we have omitted from the tabulation; and they also disagree strongly for most weaker lines which we have, therefore, not included. The work by Nussbaumer and Swings can thus essentially be regarded as a check of Garstang's earlier calculations. It is, however, confined to magnetic dipole lines, while for electric quadrupole lines only Garstang's values are available.

In selecting the tabulated lines from Garstang's tables, we have attempted to present all those lines which are observed to be at least fairly strong. These account generally for about 95 percent of the intensity of the lines within a multiplet and also about 95 percent of the radiative de-excitation from a given upper level. The majority of the lines is predominantly due to either electric quadrupole or magnetic dipole radiation. This is then the only type of transition listed. However, if

the two types of radiation contribute comparably to the total intensity of a line, then both components are given.

Numerous comparisons have been made by Thackeray [46] between Garstang's calculated $g_k A_{ki}$ -values and astrophysically observed intensities. The comparisons are for the lines within the multiplets, and the agreement is usually quite impressive. Several representative sample comparisons are given in the General Introduction.

[Fe II]

No.	Multiplet	$\lambda(\text{\AA})$	$E_i(\text{cm}^{-1})$	$E_k(\text{cm}^{-1})$	g_i	g_k	Type of transition	$A_{ki}(\text{s}^{-1})$
1.	a^6D-a^6D	2598.20	0.00	384.77	10	8	<i>m</i>	0.0021
		3534.20	384.77	667.64	8	6	<i>m</i>	0.0016
		5127.10	667.64	862.63	6	4	<i>m</i>	7.2(-4)*
		8738.90	862.63	977.03	4	2	<i>m</i>	1.9(-4)
2.	a^6D-b^4P (4F)	4889.63	385	20831	8	6	<i>m</i>	0.36
		4728.07	668	21812	6	4	<i>m</i>	0.48
		4639.68	863	22410	4	2	<i>m</i>	0.49
		4772.07	863	21812	4	4	<i>m</i>	0.026
		4664.45	977	22410	2	2	<i>m</i>	0.15
		5006.65	863	20831	4	6	<i>m</i>	0.027
		4798.28	977	21812	2	4	<i>m</i>	0.082
3.	a^6D-b^4F (6F)	4416.27	0	22637	10	10	<i>m</i>	0.46
		4457.95	385	22810	8	8	<i>m</i>	0.29
		4488.75	668	22939	6	6	<i>m</i>	0.15
		4509.61	863	23031	4	4	<i>m</i>	0.058
		4382.75	0	22810	10	8	<i>m</i>	0.055
		4432.45	385	22939	8	6	<i>m</i>	0.054
		4470.29	668	23031	6	4	<i>m</i>	0.029
		4492.64	385	22637	8	10	<i>m</i>	0.060
		4514.90	668	22810	6	8	<i>m</i>	0.066
		4528.39	863	22939	4	6	<i>m</i>	0.046
		4533.00	977	23031	2	4	<i>m</i>	0.016
		4287.40	0	23318	10	6	<i>e</i>	1.1
		4359.34	385	23318	8	6	<i>e</i>	0.82
4.	a^6D-a^6S (7F)	4413.78	668	23318	6	6	<i>e</i>	0.58
		4452.11	863	23318	4	6	<i>e</i>	0.37
		4474.91	977	23318	2	6	<i>e</i>	0.18
		3175.38	0	31483	10	8	<i>m</i>	0.22
5.	a^6D-b^4D (11F)	3224.54	385	31388	8	6	<i>m</i>	0.046
		3277.12	668	31368	4	2	<i>m</i>	0.041
		3214.67	385	31483	8	8	<i>m</i>	0.069
		3254.24	668	31388	6	6	<i>m</i>	0.12
		3277.55	863	31364	4	4	<i>m</i>	0.16
		3209.46	977	31368	2	2	<i>m</i>	0.22
		3244.18	668	31483	6	8	<i>m</i>	0.029
		3275.02	863	31388	4	6	<i>m</i>	0.056
		3289.89	977	31364	2	4	<i>m</i>	0.061
		179330	1872.60	2430.08	10	8	<i>m</i>	0.0058
6.	a^4F-a^4F	245120	2430.08	2837.94	8	6	<i>m</i>	0.0039
		357630	2837.94	3117.48	6	4	<i>m</i>	0.0014
		8616.96	1873	13474	10	6	<i>e</i>	0.017
		8891.88	2430	13673	8	4	<i>e</i>	0.010
		9033.45	2838	13905	6	2	<i>e</i>	0.0075
		9051.92	2430	13474	8	6	<i>e</i>	0.0039
		9226.60	2838	13673	6	4	<i>e</i>	0.0060
7.	a^4F-a^4P (13F)	9267.54	3117	13905	4	2	<i>e</i>	0.0099
		9470.93	3117	13673	4	4	<i>e</i>	0.0017

[Fe II]—Continued

No.	Multiplet	$\lambda(\text{\AA})$	$E_i(\text{cm}^{-1})$	$E_k(\text{cm}^{-1})$	g_i	g_k	Type of transition	$A_{ki}(\text{s}^{-1})$
8.	a^4F-a^2G (14F)	7155.14	1873	15845	10	10	<i>m</i>	0.15
		7171.98	2430	16369	8	8	<i>m</i>	0.056
		6896.18	1873	16369	10	8	<i>m</i>	0.0052
		7452.50	2430	15845	8	10	<i>m</i>	0.048
		7388.16	2838	16369	6	8	<i>m</i>	0.043
9.	a^4F-b^4P (18F)	5273.38	1873	20831	10	6	<i>e</i>	0.37
		5158.00	2430	21812	8	4	<i>e</i>	0.30
		5107.95	2838	22410	6	2	<i>e</i>	0.24
		5433.15	2430	20831	8	6	<i>e</i>	0.11
		5268.88	2838	21812	6	4	<i>e</i>	0.19
		5181.97	3117	22410	4	2	<i>e</i>	0.34
		5556.31	2838	20831	6	6	<i>e</i>	0.022
10.	a^4F-a^4H (19F)	5158.81	1873	21252	10	14	<i>e</i>	0.44
		5261.61	2430	21430	8	12	<i>e</i>	0.31
		5333.65	2838	21582	6	10	<i>e</i>	0.26
		5376.47	3117	21712	4	8	<i>e</i>	0.26
		5111.63	1873	21430	10	12	<i>e</i>	0.10
		5220.06	2430	21582	8	10	<i>e</i>	0.11
		5296.84	2838	21712	6	8	<i>e</i>	0.091
		5072.40	1873	21582	10	10	<i>e</i>	0.022
		5184.80	2430	21712	8	8	<i>e</i>	0.021
		4814.55	1873	22637	10	10	<i>e</i>	0.40
11.	a^4F-b^4F (20F)	4905.35	2430	22810	8	8	<i>e</i>	0.22
		4973.39	2838	22939	6	6	<i>e</i>	0.14
		5020.24	3117	23031	4	4	<i>e</i>	0.18
		4774.74	1873	22810	10	8	<i>e</i>	0.13
		4874.49	2430	22939	8	6	<i>e</i>	0.17
		4950.74	2838	23031	6	4	<i>e</i>	0.17
		4947.38	2430	22637	8	10	<i>e</i>	0.050
		5005.52	2838	22810	6	8	<i>e</i>	0.071
		5043.53	3117	22939	4	6	<i>e</i>	0.065
		4745.49	1873	22939	10	6	<i>e</i>	0.013
		4852.73	2430	23031	8	4	<i>e</i>	0.022
		4243.98	1873	25429	10	12	<i>e</i>	0.90
		4276.83	2430	25805	8	10	<i>e</i>	0.65
12.	a^4F-a^4G (21F)	4319.62	2838	25982	6	8	<i>e</i>	0.53
		4358.37	3117	26055	4	6	<i>e</i>	0.73
		4177.21	1873	25805	10	10	<i>e</i>	0.14
		4244.81	2430	25982	8	8	<i>e</i>	0.25
		4305.90	2838	26055	6	6	<i>e</i>	0.31
		4231.56	2430	26055	8	6	<i>e</i>	0.024
		4346.85	2430	25429	8	12	<i>e</i>	0.21
		4352.78	2838	25805	6	10	<i>e</i>	0.31
		4372.43	3117	25982	4	8	<i>e</i>	0.28
		4356.14	2838	25700	6	4	<i>c</i>	0.0080
13.	a^4F-b^2P (22F)	4197.81	3117	26933	4	2	<i>e</i>	0.0099
		4280.0	2430	25788	8	4	<i>e</i>	0.0017
		4149.1	2838	26933	6	2	<i>e</i>	0.0021
		4409.86	3117	25788	4	4	<i>e</i>	0.0042
		4114.48	1873	26170	10	12	<i>e</i>	0.045
14.	a^4F-b^2H (23F)	4178.95	2430	26353	8	10	<i>e</i>	0.0051
		4211.1	2430	26170	8	12	<i>e</i>	0.024
		4251.4	2838	26353	6	10	<i>e</i>	0.0087
		4083.78	1873	26353	10	10	<i>e</i>	0.0030
		3505.81	1873	30389	10	10	<i>e</i>	0.0032
15.	a^4F-b^2G (25F)	3528.28	2430	30764	8	8	<i>e</i>	0.0022
		3575.72	2430	30389	8	10	<i>e</i>	0.0028
		3579.81	2838	30764	6	8	<i>e</i>	0.0016
		3628.65	2838	30389	6	10	<i>e</i>	0.0011

[Fe II]--Continued

No.	Multiplet	$\lambda(\text{\AA})$	$E_i(\text{cm}^{-1})$	$E_k(\text{cm}^{-1})$	g_i	g_k	Type of transition	$A_{ki}(\text{s}^{-1})$
16.	a^4F-b^4D (26F)	3376.20	1873	31483	10	8	e	0.73
		3452.30	2430	31388	8	6	e	0.37
		3504.51	2838	31364	6	4	e	0.21
		3538.69	3117	31368	4	2	e	0.40
		3387.10	1873	31388	10	6	e	0.20
		3455.11	2430	31364	8	4	e	0.36
		3504.02	2838	31368	6	2	e	0.52
		3440.99	2430	31483	8	8	e	0.24
		3501.62	2838	31388	6	6	e	0.34
		3539.19	3117	31364	4	4	e	0.38
17.	a^4F-b^2F (27F)	3318.38	1873	31999	10	8	m	0.042
		3402.50	2430	31812	8	6	m	0.012
		3380.95	2430	31999	8	8	m	0.0062
		3450.39	2838	31812	6	6	m	0.0087
		3428.24	2838	31999	6	8	m	0.017
18.	a^4D-b^4P (30F)	7764.69	7955	20831	8	6	m	0.028
		7613.15	8680	21812	4	4	m	0.012
		7370.94	8847	22410	2	2	m	0.018
19.	a^4D-b^4F (31F)	6809.21	7955	22637	8	10	m	0.025
		6933.67	8392	22810	6	8	m	0.0017
		7011.24	8680	22939	4	6	m	0.0017
		7047.99	8847	23031	2	4	m	0.016
		6729.85	7955	22810	8	8	m	0.017
		6872.17	8392	22939	6	6	m	0.022
		6966.32	8680	23031	4	4	m	0.026
		6671.90	7955	22939	8	6	m	0.0044
		6829.01	8392	23031	6	4	m	0.0060
		5746.96	8392	25788	6	4	m	0.37
20.	a^4D-b^2P (34F)	5477.25	8680	26933	4	2	m	0.44
		5483.90	8680	25788	4	4	m	0.015
		5527.61	8847	26933	2	2	m	0.12
		5901.26	8847	25788	2	4	m	0.040
		5163.94	7955	27315	8	8	m	0.32
21.	a^4D-a^2F (35F)	4383.0	7955	30764	8	8	m	0.0050
		4468.6	8392	30764	6	8	m	0.0032
23.	a^4D-b^4D (36F)	4266.34	7955	31388	8	6	m	0.024
		4351.80	8392	31364	6	4	m	0.014
		4329.43	8392	31483	6	8	m	0.017
		4402.60	8680	31388	4	6	m	0.013
24.	a^4D-b^2F (37F)	4157.89	7955	31999	8	8	m	0.018
		4234.81	8392	31999	6	8	m	0.0082
25.	a^4D-b^2D	3532.8	7955	36253	8	6	m	0.20
		3604.7	8392	36126	6	4	m	0.014
		3588.2	8392	36253	6	6	m	0.038
		3642.5	8680	36126	4	4	m	0.071
		3625.7	8680	36253	4	6	m	0.058
		3664.8	8847	36126	2	4	m	0.14
26.	a^4P-a^2P	20457	13474	18361	6	4	m	0.063
		21325	13673	18361	4	4	m	0.032
		20067	13905	18887	2	2	m	0.081
		22436	13905	18361	2	4	m	0.014

[Fe II]—Continued

No.	Multiplet	$\lambda(\text{\AA})$	$E_i(\text{cm}^{-1})$	$E_k(\text{cm}^{-1})$	g_i	g_k	Type of transition	$A_{ki}(\text{s}^{-1})$
27.	a^4P-b^4F	10708	13474	22810	6	8	e	0.0016
		10789	13673	22939	4	6	e	0.0025
		10955	13905	23031	2	4	e	0.0031
		10683	13673	23031	4	4	e	0.0013
		10910	13474	22637	6	10	e	0.0039
		10942	13673	22810	4	8	e	0.0025
		11066	13905	22939	2	6	e	0.0013
28.	a^4P-b^4D (39F)	5551.31	13474	31483	6	8	e	0.13
		5725.92	13905	31364	2	4	e	0.039
		5580.82	13474	31388	6	6	e	0.13
		5650.94	13673	31364	4	4	e	0.074
		5588.15	13474	31364	6	4	e	0.072
		5649.67	13673	31368	4	2	e	0.16
		5613.3	13673	31483	4	8	e	0.073
		5718.3	13905	31388	2	6	e	0.066
		5586.9	13474	31368	6	2	e	0.020
29.	a^4P-c^2D	4082.0	13673	38164	4	6	e	0.033
30.	a^2G-b^2H (41F)	9682.13	15845	26170	10	12	e	0.013
		10013.9	16369	26353	8	10	e	0.010
		{ 9513.87	15845	26353	10	10	e m	0.0079 0.0012 }
31.	a^2G-a^2F (42F)	{ 8715.84	15845	27315	10	8	e m	0.050 0.0022 }
		8885.66	16369	27620	8	6	e	0.012
		{ 9133.63	16369	27315	8	8	e m	0.0039 0.0030 }
		8490.3	15845	27620	10	6	e	0.0049
32.	a^2G-b^2G (43F)	6873.87	15845	30389	10	10	e	0.098
		6944.91	16369	30764	8	8	e	0.087
		6700.68	15845	30764	10	8	e	0.012
		7131.13	16369	30389	8	10	e	0.011
33.	a^2G-b^2F (44F)	{ 6188.55	15845	31999	10	8	e m	0.10 0.029 }
		{ 6473.86	16369	31812	8	6	e m	0.035 0.028 }
		6396.30	16369	31999	8	8	m	0.045
		6261.2	15845	31812	10	6	e	0.014
34.	a^2G-a^2I	5870.0	15845	32076	10	14	e	0.14
		6043.9	16369	32910	8	12	e	0.11
35.	a^2G-c^2G	5673.2	15845	33467	10	10	e	0.30
		5855.4	16369	33501	8	8	e	0.32
		5847.0	16369	33467	8	10	e	0.033
36.	a^2G-b^2D	5027.8	16369	36253	8	6	e	0.087
		4898.7	15845	36253	10	6	e	0.82
		5060.1	16369	36126	8	4	e	0.63
37.	a^2G-c^2D	4479.2	15845	38164	10	6	e	0.24
		4576.2	16369	38215	8	4	e	0.48
38.	a^2P-a^2F (45F)	10796.5	18361	27620	4	6	e	0.0021
		11165	18361	27315	4	8	e	0.0070
		11448	18887	27620	2	6	e	0.0026
39.	a^2P-b^2F (47F)	7432.23	18361	31812	4	6	e	0.0059
		7330.4	18361	31999	4	8	e	0.0014
		7734.8	18887	31812	2	6	e	0.0044

[Fe II]—Continued

No.	Multiplet	$\lambda(\text{\AA})$	$E_i(\text{cm}^{-1})$	$E_k(\text{cm}^{-1})$	g_i	g_k	Type of transition	$A_{ki}(\text{s}^{-1})$
40.	a^2P-b^2D	5587.5	18361	36253	4	6	e	0.036
		5799.2	18887	36126	2	4	e	0.081
		5627.5	18361	36126	4	4	e	0.15
		5756.8	18887	36253	2	6	e	0.018
41.	a^2P-c^2D	5048.3	18361	38164	4	6	e	0.42
		5172.4	18887	38215	2	4	e	0.21
		5035.4	18361	38215	4	4	e	0.11
		5186.1	18887	38164	2	6	e	0.11
42.	a^2H-b^2H	17148	20340	26170	12	12	e	0.0026
		18023	20806	26353	10	10	e	0.0020
43.	a^2H-b^2C (48F)	9949.32	20340	30389	12	10	e	0.021
		10038.8	20806	30764	10	8	e	0.019
		10432.6	20806	30389	10	10	m	0.0016
		9590.6	20340	30764	12	8	e	0.0016
44.	a^2H-b^2F (49F)	8931.47	20806	31999	10	8	e	0.0034
		8574.7	20340	31999	12	8	e	0.031
		9083.5	20806	31812	10	6	e	0.030
45.	a^2H-a^2I	7974.8	20340	32876	12	14	e	0.069
		8259.5	20806	32910	10	12	e	0.060
46.	a^2D-b^2G (50F)	10127	20517	30389	6	10	e	0.0076
		10572	21308	30764	4	6	e	0.0067
47.	a^2D-c^2G	7719.9	20517	33467	6	10	e	0.029
		8199.2	21308	33501	4	8	c	0.019
48.	a^2D-b^2D	6353.1	20517	36253	6	6	e	0.17
		6746.7	21308	36126	4	4	e	0.056
		6404.8	20517	36126	6	4	e	0.062
		6689.4	21308	36253	4	6	e	0.043
49.	a^2D-a^2S	5982.8	20517	37227	6	2	e	0.25
		6280.1	21308	37227	4	2	e	0.17
50.	a^2D-c^2D	5913.1	21308	38215	4	4	e	0.090
51.	b^4P-b^2P	25144	21812	25788	4	4	m	0.015
		22103	22410	26933	2	2	m	0.024
		20168	20831	25788	6	4	m	0.043
		19522	21812	26933	4	2	m	0.0049
		29595	22410	25788	2	4	m	0.0064
52.	b^4P-b^4D	9385.3	20831	31483	6	8	m	0.055
		9469.8	20831	31388	6	6	m	0.030
		10466	21812	31364	4	4	m	0.043
		11160	22410	31368	2	2	m	0.057
		9491.4	20831	31364	6	4	m	0.021
		10462	21812	31368	4	2	m	0.037
53.	b^4P-b^2D	6482.5	20831	36253	6	6	m	0.042
		6922.8	21812	36253	4	6	m	0.010
54.	b^4P-a^2S	6485.4	21812	37227	4	2	m	0.73
		6747.1	22410	37227	2	2	m	0.20
55.	b^4P-c^2D	5767.7	20831	38164	6	6	m	0.082
		6094.8	21812	38215	4	4	m	0.047

[Fe II]—Continued

No.	Multiplet	$\lambda(\text{\AA})$	$E_i(\text{cm}^{-1})$	$E_k(\text{cm}^{-1})$	g_i	g_k	Type of transition	$A_{ki}(\text{s}^{-1})$
56.	a^4H-b^2G	11159	21430	30389	12	10	<i>m</i>	0.020
		10888	21582	30764	10	8	<i>m</i>	0.020
		11351	21582	30389	10	10	<i>m</i>	0.0045
		11044	21712	30764	8	8	<i>m</i>	0.014
57.	a^4H-a^2I	8734.3	21430	32876	12	14	<i>m</i>	0.039
		8825.3	21582	32910	10	12	<i>m</i>	0.038
		8600.5	21252	32876	14	14	<i>m</i>	0.097
		8708.4	21430	32910	12	12	<i>m</i>	0.038
		8575.5	21252	32910	14	12	<i>m</i>	0.0014
58.	a^4H-c^2G	8305.4	21430	33467	12	10	<i>m</i>	0.15
		8387.7	21582	33501	10	8	<i>m</i>	0.15
		8411.7	21582	33467	10	10	<i>m</i>	0.019
		8480.2	21712	33501	8	8	<i>m</i>	0.10
59.	b^4F-b^2G	13191	22810	30389	8	10	<i>m</i>	0.0070
		12776	22939	30764	6	8	<i>m</i>	0.0073
		12896	22637	30389	10	10	<i>m</i>	0.020
		12569	22810	30764	8	8	<i>m</i>	0.0065
60.	b^4F-b^4D	11655	22810	31388	8	6	<i>m</i>	0.048
61.	b^4F-c^2G	9380.9	22810	33467	8	10	<i>m</i>	0.070
		9465.3	22939	33501	6	8	<i>m</i>	0.065
		9231.1	22637	33467	10	10	<i>m</i>	0.21
		9351.1	22810	33501	8	8	<i>m</i>	0.10
		9202.2	22637	33501	10	8	<i>m</i>	0.013
62.	b^4F-c^2D	6511.2	22810	38164	8	6	<i>m</i>	0.16
		6544.4	22939	38215	6	4	<i>m</i>	0.19
		6566.3	22939	38164	6	6	<i>m</i>	0.022
		6584.1	23031	38215	4	4	<i>m</i>	0.11
63.	b^2P-b^4D	17852	25788	31388	4	6	<i>m</i>	0.011
		22562	26933	31364	2	4	<i>m</i>	0.014
64.	b^2P-b^2D	9553.1	25788	36253	4	6	<i>m</i>	0.022
		10875	26933	36126	2	4	<i>m</i>	0.015
		9670.4	25788	36126	4	4	<i>m</i>	0.075
65.	b^2P-a^2S	8739.6	25788	37227	4	2	<i>m</i>	0.23
		9711.7	26933	37227	2	2	<i>m</i>	0.23
66.	b^2P-c^2D	8077.9	25788	38164	4	6	<i>m</i>	0.021
		8861.3	26933	38215	2	4	<i>m</i>	0.013
		8044.8	25788	38215	4	4	<i>m</i>	0.030
67.	b^2H-b^2C	23696	26170	30389	12	10	<i>m</i>	0.019
		22664	26353	30764	10	8	<i>m</i>	0.019
		24770	26353	30389	10	10	<i>m</i>	0.027
68.	b^2H-a^2I	14908	26170	32876	12	14	<i>m</i>	0.016
		15247	26353	32910	10	12	<i>m</i>	0.013
		14833	26170	32910	12	12	<i>m</i>	0.031
69.	b^2H-c^2G	13701	26170	33467	12	10	<i>m</i>	0.034
		13986	26353	33501	10	8	<i>m</i>	0.036
		14053	26353	33467	10	10	<i>m</i>	0.065
70.	a^2F-c^2G	16250	27315	33467	8	10	<i>m</i>	0.037
		16999	27620	33501	6	8	<i>m</i>	0.012
		16161	27315	33501	8	8	<i>m</i>	0.073
71.	a^2F-c^2D	9435.8	27620	38215	6	4	<i>m</i>	0.045

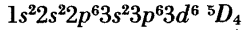
[Fe II]—Continued

No.	Multiplet	$\lambda(\text{\AA})$	$E_i(\text{cm}^{-1})$	$E_k(\text{cm}^{-1})$	g_i	g_k	Type of transition	$A_{ki}(\text{s}^{-1})$
72.	$b\ ^4D - c\ ^2D$	14964	31483	38164	8	6	<i>m</i>	0.029
		14601	31368	38215	2	4	<i>m</i>	0.027

*The number in parentheses following the tabulated value indicates the power of ten by which this value has to be multiplied.

[Fe III]

Ground State
Ionization Potential



$$247221 \text{ cm}^{-1} = 30.651 \text{ eV}$$

List of tabulated lines

Wavelength [Å]	No.*	Wavelength [Å]	No.*
3236.7	6	4667.0	3
3239.7	5	4701.62	3
3286.2	5	4733.93	3
3301.6	5	4754.83	3
3319.2	5	4769.60	3
3333.8	5	4777.88	3
3334.9	5	4881.11	2
3355.9	5	4930.5	1
3356.6	5	5011.3	1
3366.2	5	5084.8	1
4008.3	4	5270.3	1
4046.4	4	5412.0	1
4079.7	4	6096.3	8
4096.6	4	6614.0	8
4607.13	3	7078.2	7
4658.10	3		

*The numbers in the lists of tabulated lines refer to the running multiplet numbers of the tables. ("Lists of tabulated lines" have been given for all spectra where 20 or more lines have been tabulated.)

All our data are taken from the extensive calculations of Garstang [5]. From his much larger tables, we have

listed here only the relatively strong lines, which are all due predominantly (> 99%) to magnetic dipole radiation and amount to about one-sixth of his total list. It is difficult to make an assessment of the uncertainties in these theoretical data. The nature of the calculations precludes quantitative estimates of the uncertainties, and no direct experimental comparison data are available for the forbidden lines of any of the heavy-element spectra. However, for this spectrum Garstang could assemble in his paper some astrophysical observational intensity data for the lines of a fairly prominent multiplet (our running number 3), and he has found a surprisingly close agreement between the astrophysical intensities and his calculated line intensities. This good agreement, as well as similar good agreement with astrophysical observations for the spectra of [Fe II] and [Ni II] (see General Introduction) and our previous experience with the evaluation of forbidden line data on simpler atoms, suggests that the strengths of the listed stronger lines should be accurate to within a factor of two. We expect, on the other hand, that larger uncertainties will be encountered in the weaker lines which are not included in our tabulation.

[Fe III]

No.	Multiplet	$\lambda(\text{\AA})$	$E_i(\text{cm}^{-1})$	$E_k(\text{cm}^{-1})$	g_i	g_k	Type of transition	$A_{ki}(\text{s}^{-1})$
1.	$a\ ^5D - a\ ^3P$ (1F)	5270.3	436	19405	7	5	<i>m</i>	0.40
		5011.3	739	20688	5	3	<i>m</i>	0.53
		4930.5	932	21209	3	1	<i>m</i>	0.67
		5412.0	932	19405	3	5	<i>m</i>	0.038
		5084.8	1027	20688	1	3	<i>m</i>	0.091
2.	$a\ ^5D - a\ ^3H$ (2F)	4881.11	0	20482	9	9	<i>m</i>	0.0048
3.	$a\ ^5D - a\ ^3F$ (3F)	4658.10	0	21462	9	9	<i>m</i>	0.44
		4701.62	436	21700	7	7	<i>m</i>	0.27
		4733.93	739	21857	5	5	<i>m</i>	0.10
		4607.13	0	21700	9	7	<i>m</i>	0.038
		4667.0	436	21857	7	5	<i>m</i>	0.026
		4754.83	436	21462	7	9	<i>m</i>	0.081
		4769.60	739	21700	5	7	<i>m</i>	0.087
		4777.88	932	21857	3	5	<i>m</i>	0.049

[Fe III]—Continued

No.	Multiplet	$\lambda(\text{\AA})$	$E_i(\text{cm}^{-1})$	$E_k(\text{cm}^{-1})$	g_i	g_k	Type of transition	$A_{ki}(\text{s}^{-1})$
4.	a^5D-a^3G (4F)	4079.7	436	24941	7	9	<i>m</i>	0.0037
		4096.6	739	25142	5	7	<i>m</i>	0.0027
		4008.3	0	24941	9	9	<i>m</i>	0.019
		4046.4	436	25142	7	7	<i>m</i>	0.0080
5.	a^5D-a^3D (6F)	3239.7	0	30858	9	7	<i>m</i>	0.23
		3301.6	436	30716	7	5	<i>m</i>	0.027
		3333.8	739	30726	5	3	<i>m</i>	0.0013
		3286.2	436	30858	7	7	<i>m</i>	0.047
		3334.9	739	30716	5	5	<i>m</i>	0.11
		3355.9	932	30726	3	3	<i>m</i>	0.015
		3319.2	739	30858	5	7	<i>m</i>	0.044
		3356.6	932	30716	3	5	<i>m</i>	0.095
		3366.2	1027	30726	1	3	<i>m</i>	0.13
		3236.7	0	30886	9	9	<i>m</i>	0.0022
7.	a^3P-a^1S (9F)	7078.2	20688	34812	3	1	<i>m</i>	1.5
8.	a^3P-a^1D (10F)	6096.3 6614.0	19405 20688	35804 35804	5 3	5 5	<i>m</i> <i>m</i>	0.096 0.033

[Fe IV]

Ground State
Ionization Potential $1s^2 2s^2 2p^6 3s^2 3p^6 3d^5 6S_{5/2}$
[442000] $\text{cm}^{-1} = [54.8] \text{ eV}$

List of tabulated lines

Wavelength [Å]	No.*	Wavelength [Å]	No.*
4144.4	3	4918.1	2
4152.5	3	5032.3	1
4206.5	3	5033.8	1
4214.9	3	5233.2	1
4217.1	3	5235.1	1
4866.2	2	5236.6	1
4867.8	2	7109.7	4
4868.2	2	7170.6	4
4869.2	2	7183.0	4
4869.6	2	7189.4	4
4889.1	2	7190.4	4
4900.5	2	7191.2	4
4903.5	2	7192.2	4
4906.7	2	7220.9	4

* The numbers in the lists of tabulated lines refer to the running multiplet numbers of the tables. ("Lists of tabulated lines" have been given for all spectra where 20 or more lines have been tabulated.)

The listed data are taken from 1958 calculations by Garstang [6]. We have selected from this paper all lines of at least moderate strength, the majority of which are due to magnetic dipole radiation. At the time of Garstang's calculations, no observational analysis of the [Fe IV] spectrum existed, and therefore, no precise wavelengths for the forbidden lines were available. In the meantime, Edlén [48] completed an energy level analysis of this spectrum, and we could utilize the wavelengths from his paper. For the tabulated transitions, the wavelength changes compared with Garstang's calculated values turned out to be quite small, the largest about 4 percent. We have therefore not made any corrections in the transition probabilities due to the changed wavelengths. We estimate the uncertainties for this spectrum to be slightly higher than for [Fe III] or [Fe V], since the $3d^5$ configuration (i.e., half-filled shell) is the most complex in the $3d$ shell. A more detailed discussion on the assessment of the accuracy of forbidden transition probabilities is presented in the General Introduction.

[Fe IV]

No.	Multiplet	$\lambda(\text{\AA})$	$E_i(\text{cm}^{-1})$	$E_k(\text{cm}^{-1})$	g_i	g_k	Type of transition	$A_{ki}(\text{s}^{-1})$
1.	a^4G-a^2F	5233.2	32293	51396	10	8	<i>m</i>	0.50
		5033.8	32305	52166	8	6	<i>m</i>	0.47
		5236.6	32305	51396	8	8	<i>m</i>	0.080
		5032.3	32300	52166	6	6	<i>m</i>	0.21
		5235.1	32300	51396	6	8	<i>m</i>	0.015

[Fe IV]—Continued

No.	Multiplet	$\lambda(\text{\AA})$	$E_i(\text{cm}^{-1})$	$E_k(\text{cm}^{-1})$	g_i	g_k	Type of transition	$A_{ki}(\text{s}^{-1})$
2.	a^4G-a^4F	4906.7	32246	52620	12	10	<i>m</i>	0.11
		{ 4900.5	32293	52694	10	8	<i>e</i>	0.21 }
		{ 4869.2	32305	52837	8	6	<i>m</i>	0.039
		{ 4868.2	32300	52835	6	4	<i>e</i>	0.15
		{ 4918.1	32293	52620	10	10	<i>m</i>	0.11
		{ 4903.5	32305	52694	8	8	<i>m</i>	0.14 }
		{ 4867.8	32300	52837	6	6	<i>e</i>	0.18 }
		{ 4889.1	32246	52694	12	8	<i>e</i>	0.073 }
		{ 4866.2	32293	52837	10	6	<i>e</i>	0.045
		{ 4869.6	32305	52835	8	4	<i>e</i>	0.067
		4152.5	32293	56368	10	12	<i>m</i>	0.061
		4217.1	32305	56012	8	10	<i>m</i>	0.13
		4144.4	32246	56368	12	12	<i>m</i>	0.47
3.	a^4G-a^2H	4214.9	32293	56012	10	10	<i>m</i>	0.042
		4206.5	32246	56012	12	10	<i>m</i>	0.056
4.	a^4D-a^4F	{ 7220.9	38776	52620	8	10	<i>m</i>	0.14 }
		{ 7191.2	38935	52837	4	6	<i>e</i>	0.023 }
		{ 7170.6	38893	52835	2	4	<i>m</i>	0.10
		{ 7183.0	38776	52694	8	8	<i>m</i>	0.10 }
		{ 7189.4	38932	52837	6	6	<i>e</i>	0.011 }
		{ 7192.2	38935	52835	4	4	<i>m</i>	0.18 }
		{ 7109.7	38776	52837	8	6	<i>e</i>	0.012 }
		{ 7190.4	38932	52835	6	4	<i>m</i>	0.16 }
		{ 7109.7	38776	52837	8	6	<i>m</i>	0.098
		{ 7190.4	38932	52835	6	4	<i>m</i>	0.039

[Fe V]

Ground State
Ionization Potential $1s^2 2s^2 2p^6 3s^2 3p^6 3d^4 \text{ } ^5D_0$
[604900] cm^{-1} = [75.0] eV

All the listed data are taken from the calculations by Garstang [5]. We have presented only the lines of at least moderate strength, which amount to about one-sixth of his magnetic dipole lines. The listed lines are primarily due to magnetic dipole radiation, since the electric quadrupole component is negligible. As for [Fe III], we estimate the uncertainties for the listed prom-

inent lines to be less than a factor of two. A good indication that this is a reasonable estimate comes from the good agreement between the calculated values and a few astrophysical observations which are available for the spectra of [Fe II], [Fe III], and [Ni II] (see General Introduction).

[Fe V]

No.	Multiplet	$\lambda(\text{\AA})$	$E_i(\text{cm}^{-1})$	$E_k(\text{cm}^{-1})$	g_i	g_k	Type of transition	$A_{ki}(\text{s}^{-1})$
1.	a^5D-a^3P (1F)	3895.52	804	26466	7	5	<i>m</i>	0.71
		4071.29	419	24973	5	3	<i>m</i>	1.1
		4180.87	145	24054	3	1	<i>m</i>	1.3
		3798.2	145	26466	3	5	<i>m</i>	0.036
		4003.2	0	24973	1	3	<i>m</i>	0.13
2.	a^5D-a^3H (2F)	4227.49	1285	24937	9	9	<i>m</i>	0.0011

[Fe v]—Continued

No.	Multiplet	$\lambda(\text{\AA})$	$E_i(\text{cm}^{-1})$	$E_k(\text{cm}^{-1})$	g_i	g_k	Type of transition	$A_{ki}(\text{s}^{-1})$
3.	a^5D-a^3F (3F)	3891.28	1285	26973	9	9	<i>m</i>	0.74
		3839.52	804	26846	7	7	<i>m</i>	0.40
		3795.23	419	26765	5	5	<i>m</i>	0.20
		3911.86	1285	26846	9	7	<i>m</i>	0.066
		3851.35	804	26765	7	5	<i>m</i>	0.047
		3820.2	804	26973	7	9	<i>m</i>	0.16
		3783.56	419	26846	5	7	<i>m</i>	0.16
4.	a^5D-a^3G (4F)	3406.6	804	30150	7	9	<i>m</i>	0.0078
		3400.3	419	29820	5	7	<i>m</i>	0.0070
		3463.4	1285	30150	9	9	<i>m</i>	0.032
		3445.4	804	29820	7	7	<i>m</i>	0.017
		3503.5	1285	29820	9	7	<i>m</i>	0.0026

[Fe vi]

List of tabulated lines

Wavelength [Å]	No.*	Wavelength [Å]	No.*
3494.7	4	4968.8	2
3511.6	4	4972.1	2
3558.1	4	5100.4	1
3575.6	4	5145.77	2
3630.3	5	5176.43	2
3645.7	4	5236.6	1
3664.1	4	5279.2	1
3740.2	5	5335.23	1
3774.9	3	5370.5	2
3776.1	4	5423.9	1
3815.1	3	5426.6	1
3849.1	3	5484.78	1
3890.9	3	5630.82	1
3995.8	3	5676.96	1

*The numbers in the lists of tabulated lines refer to the running multiplet numbers of the tables. ("Lists of tabulated lines" have been given for all spectra where 20 or more lines have been tabulated.)

[Fe vi]

No.	Multiplet	$\lambda(\text{\AA})$	$E_i(\text{cm}^{-1})$	$E_k(\text{cm}^{-1})$	g_i	g_k	Type of transition	$A_{ki}(\text{s}^{-1})$
1.	a^4F-a^4P (1F)	5676.96	1994	19601	10	6	<i>e</i>	0.048
		5630.82	1185	18937	8	4	<i>e</i>	0.036
		5484.78	510	18734	6	2	<i>e</i>	0.031
		{ 5426.6	1185	19601	8	6	<i>m</i>	0.0020
		{ 5423.9	510	18937	6	4	<i>m</i>	0.0010
		{ 5335.23	0	18734	4	2	<i>e</i>	0.055
		{ 5236.6	510	19601	6	6	<i>e</i>	0.0053
		{ 5279.2	0	18937	4	4	<i>m</i>	0.0020
		{ 5100.4	0	19601	4	6	<i>e</i>	0.012
		{ 5176.43	1994	21305	10	10	<i>m</i>	6.5(-4)*
		{ 5145.77	1185	20609	8	8	<i>m</i>	0.22
2.	a^4F-a^2G (2F)	5370.5	1994	20609	10	8	<i>m</i>	0.012
		4968.8	1185	21305	8	10	<i>m</i>	0.22
		4972.1	510	20609	6	8	<i>m</i>	0.20

[Fe VI]—Continued

No.	Multiplet	$\lambda(\text{\AA})$	$E_i(\text{cm}^{-1})$	$E_k(\text{cm}^{-1})$	g_i	g_k	Type of transition	$A_{ki}(\text{s}^{-1})$
3.	a^4F-a^2P (3F)	3995.8	1185	26204	8	4	e	0.0036
		3849.1	510	26483	6	2	e	0.0010
		3890.9	510	26204	6	4	m	0.42
		3774.9	0	26483	4	2	m	0.0022
		3815.1	0	26204	4	4	e	0.0012
							e	0.0013
4.	a^4F-a^2D (4F)	3776.1	1994	28469	10	6	e	4.3(-4)
		3645.7	1185	28607	8	4	e	0.0013
		3664.1	1185	28469	8	6	m	0.95
		3558.1	510	28607	6	4	m	0.68
		3575.6	510	28469	6	6	m	0.12
		3494.7	0	28607	4	4	m	0.37
		3511.6	0	28469	4	6	m	0.045
5.	a^4F-a^2H (5F)	3630.3	1185	28723	8	10	m	0.0033
		3740.2	1994	28723	10	10	m	0.0056

* The number in parentheses following the tabulated value indicates the power of ten by which this value has to be multiplied.

[Fe VII]

Ground State
Ionization Potential

$1s^22s^22p^63s^23p^63d^2\ 3F_2$
[1008000] cm $^{-1}$ = [125.0] eV

The data are taken from the work of Warner and Kirkpatrick [19]. These calculations are based on scaled Thomas-Fermi wave functions in a single-configuration approximation. The results are estimated to be reliable to within a factor of two based on comparisons with

other nearby ions. For a more detailed discussion of the accuracy of these transition probabilities and several comparisons with observations, we refer to the General Introduction.

[Fe VII]

No.	Multiplet	$\lambda(\text{\AA})$	$E_i(\text{cm}^{-1})$	$E_k(\text{cm}^{-1})$	g_i	g_k	Type of transition	$A_{ki}(\text{s}^{-1})$
1.	a^3F-a^1D (1F)	6598.8	2327	17475	9	5	e	0.0011
		6086.92	1047	17475	7	5	m	0.49
		5721.11	0	17475	5	5	m	0.31
2.	a^3F-a^3P (2F)	5277.67	2327	21275	9	5	e	0.043
		5158.98	1047	20428	7	3	e	0.045
		4989.4	0	20037	5	1	e	0.080
		4944.0	1047	21275	7	5	m	0.042
		4893.4	0	20428	5	3	e	0.016
		4699.0	0	21275	5	5	m	0.0012
3.	a^3F-a^1G (3F)	3759.9	2327	28915	9	9	m	0.37
		3587.2	1047	28915	7	9	m	0.26
4.	a^1D-a^3P	26310	17475	21275	5	5	m	0.13
		33850	17475	20428	5	3	m	0.037

[Fe VIII]

We do not list transition probabilities for this ion since no wavelengths for forbidden lines have been observed. However, calculations of some transition probabilities

and energy eigenvalues can be found in the paper of Czyzak and Krueger [30].

[Fe IX]

Ground State

 $1s^2 2s^2 2p^6 3s^2 3p^6 1S_0$

Ionization Potential

 $1895800 \text{ cm}^{-1} = 235.04 \text{ eV}$

The values for the ten visible transitions are taken from the recent calculations of Wagner and House [31]. These calculations are based on self-consistent field wave functions with modifications to account for experimental observations. Due to the approximate nature of the calculations, the results are estimated to be reliable to within a factor of two. Based on the results of this study, the authors propose identifications for several coronal lines, which, however, can only be considered tentative.

Garstang [17] has also calculated de-excitation by

magnetic quadrupole radiation from some of the same upper states which give rise to the lines that Wagner and House investigated. His results indicate de-excitation by magnetic quadrupole radiation is the dominant mechanism only for the $4s^3P_2^o$ level. Again, his data should be reliable to within a factor of two.

With the exception of the $4s^3P_2^o$ level, the energy level data are taken from Wagner and House's calculations [31]. This necessitated modifying Garstang's results for the $3p^6 1S_0 - 3p^5 3d$, $3P_2^o$, $3F_2^o$ transitions to account for the change in wavelength.

[Fe IX]

No.	Transition array	Multiplet	$\lambda(\text{\AA})$	$E_i(\text{cm}^{-1})$	$E_k(\text{cm}^{-1})$	g_i	g_k	Type of transition	$A_{ki}(\text{s}^{-1})$	Accuracy	Source
1.	$3p^6 - 3p^5 3d$	$1S - 3P^o$	246	0	[405873]	1	5	mq	75	DE	17n
2.		$1S - 3F^o$	235	0	[426282]	1	5	mq	0.86	DE	17n
3.		$1S - 1D^o$	222	0	[449709]	1	5	mq	27	DE	17
4.		$1S - 3D^o$	220	0	[454828]	1	5	mq	9.1	DE	17
5.	$3p^6 - 3p^5 4s$	$1S - 3P^o$	105.8	0	[945180]	1	5	mq	430	DE	17
6.	$3p^5 3d - 3p^5 3d$	$3F^o - 3D^o$	3036	[421894]	[454828]	7	5	m	6.2	DE	31
7.			3879	[421894]	[447675]	7	7	m	0.66	DE	31
8.			3503	[426282]	[454020]	5	5	m	9.2	DE	31
9.			4674	[426282]	[447675]	5	7	m	2.7	DE	31
10.		$3F^o - 1D^o$	3595	[421894]	[449709]	7	5	m	27	DE	31
11.			4269	[426282]	[449709]	5	5	m	23	DE	31
12.		$3F^o - 1F^o$	3148	[426282]	[458051]	5	7	m	17	DE	31
13.		$3D^o - 3D^o$	13981	[447675]	[454828]	7	5	m	3.8	DE	31
14.		$3D^o - 1F^o$	9638	[447675]	[458051]	7	7	m	7.2	DE	31
15.		$1D^o - 1F^o$	11988	[449709]	[458051]	5	7	m	1.6	DE	31

[Fe X] - [Fe XV]

Ion	Ground state	Ionization potential
[Fe X]	$1s^2 2s^2 2p^6 3s^2 3p^5 \ ^2P_{3/2}^o$	$2114000 \text{ cm}^{-1} = 262.1 \text{ eV}$
[Fe XI]	$1s^2 2s^2 2p^6 3s^2 3p^4 \ ^3P_2$	$2342000 \text{ cm}^{-1} = 290.4 \text{ eV}$
[Fe XII]	$1s^2 2s^2 2p^6 3s^2 3p^3 \ ^4S_{3/2}^o$	$[2668000] \text{ cm}^{-1} = [330.8] \text{ eV}$
[Fe XIII]	$1s^2 2s^2 2p^6 3s^2 3p^2 \ ^3P_0$	$[2912000] \text{ cm}^{-1} = [361.0] \text{ eV}$
[Fe XIV]	$1s^2 2s^2 2p^6 3s^2 3p^2 \ ^2P_{1/2}^o$	$[3163000] \text{ cm}^{-1} = [392.2] \text{ eV}$
[Fe XV]	$1s^2 2s^2 2p^6 3s^2 \ ^1S_0$	$3684000 \text{ cm}^{-1} = 456.7 \text{ eV}$

(a) For [Fe X] and [Fe XIV], the line strength for the one magnetic dipole transition in the ground state configuration is a straight number which has been, for example, tabulated by Krueger and Czyzak [14] (listed also in the General Introduction of our previous transition probability compilation, NSRDS-NBS 22, table 4 [2]). The quantity presented here, the transition probability, should be also quite accurate, since the energy level difference needed for the conversion from the line strength is accurately known from the wavelength observed in the solar corona. For the [Fe XIV] spectrum additional data for forbidden transition probabilities arising in excited state configurations have been calculated by Garstang [35]. We have, however, not listed these transitions since no reliable wavelengths and energy levels are known.

(b) For the spectra of [Fe XI] and [Fe XIII], calculations by Krueger and Czyzak [13] are available and have been used for this tabulation. These calculations are based on self-consistent field wave functions and include the spin-orbit and spin-spin and spin-other-orbit interactions; experimental values for the energy intervals are used whenever available.

(c) The results for [Fe XII] are taken from the very

recent calculations of Garstang [18]. Fortunately, a complete analysis of the energy levels in the ground state configuration has recently become available through identification of forbidden wavelengths in the solar corona [49, 50]. Thus Garstang [18] has recalculated the transition probabilities for transitions within the $3p^3$ configuration and finds that his new results are in very good agreement with the earlier data which were obtained by Krueger and Czyzak [14] before the complete set of energy levels was known experimentally. This agreement is particularly encouraging since [Fe XII] is a rather unfavorable case for the very highly ionized atoms. The $3p^3$ configuration, being a half-filled shell, is the most complex in the $3p$ shell, and thus the wave functions, etc., are very sensitive to the choice of the interaction parameters.

(d) For the one observed transition in [Fe XV], $\lambda = 7059 \text{ \AA}$, within the $3s3p$ configuration, calculations by Krueger and Czyzak [14] are available and have been used for this tabulation. These calculations are based on self-consistent field wave functions and include the spin-orbit and spin-spin and spin-other-orbit interactions; experimental values for the energy intervals are used whenever available. Garstang [17] has carried out "magnetic quadrupole" calculations to determine the significance of an alternative de-excitation mechanism for the upper state of the above mentioned $\lambda = 7059 \text{ \AA}$ line. It is seen that this transition, occurring at about $\lambda = 394 \text{ \AA}$, contributes only about 5 percent of the radiative de-excitations of the $^3P_2^o$ level.

(e) For some of the remaining higher stages of ionization of Fe, calculations of forbidden transition probabilities exist (see table 1 of the General Introduction). However, since only a few tentative wavelength identifications are known, we do not present any data.

[Fe X] - [Fe XV]

Ion	No.	Transition array	Multiplet	$\lambda(\text{\AA})$	$E_i(\text{cm}^{-1})$	$E_k(\text{cm}^{-1})$	g_i	g_k	Type of transition	$A_{ki}(s^{-1})$	Accuracy	Source
[Fe X]	1.	$3p^5 - 3p^5$	$^2P^o - ^2P^o$ (1F)	6374.6	0	15683	4	2	<i>m</i>	69.4	B	2, 14
[Fe XI]	1.	$3p^4 - 3p^4$	$^3P - ^3P$ (1F)	7891.8	0	12668	5	3	<i>m</i>	43	C	13
	2.		$^3P - ^1D$ (2F)	2649	0	37744	5	5	<i>m</i>	91	C	13
	3.		$^3P - ^1S$	3986.8	12268	37744	3	1	<i>m</i>	9.3	C	13
	4.		$^1D - ^1S$	1467.0	12268	80434	5	1	<i>e</i>	910	C	13
				1243.3	0	80434	5	1	<i>e</i>	1.9	D	13
	4.			2341.8	37744	80434	5	1	<i>e</i>	9.3	D	13
[Fe XII]	1.	$3p^3 - 3p^3$	$^4S^o - ^2D^o$	{ 2170	0	46083	4	6	<i>m</i>	2.1	D	18 }
				2406	0	41560	4	4	<i>e</i>	0.12	D	18 }
	2.		$^4S^o - ^2P^o$	1349.6	0	80512	4	4	<i>m</i>	53	D	18
				1242.2	0	74100	4	2	<i>m</i>	340	D	18
	3.		$^2D^o - ^2D^o$	22100	41560	46083	4	6	<i>m</i>	190	D	18
										0.87	D	18

[Fe xv]—Continued

Ion	No.	Transition array	Multiplet	$\lambda(\text{\AA})$	$E_i(\text{cm}^{-1})$	$E_k(\text{cm}^{-1})$	g_i	g_k	Type of transition	$A_{ki}(\text{s}^{-1})$	Accuracy	Source
	4.		$^2D^{\circ}-^2P^{\circ}$	{ 2903 3072	46083 41560	80512 74100	6 4	4 2	m e m e	78 1.4 69 0.91	D D D D	18 } 18 } 18 } 18 }
				2568 3568	41560 46083	80512 74100	4 6	4 2	m	200	D	18
	5.		$^2P^{\circ}-^2P^{\circ}$	15600	74100	80512	2	4	m	2.0	D	18
[Fe XIII]	1.	$3p^2-3p^2$	$^3P-^3P$ (1F)	10797.9 10746.8	9302 0	18561 9302	3 1	5 3	m m	9.7 14	C C	13 13
	2.		$^3P-^1D$ (2F)	3388.5 2580	18561 9302	48068 48068	5 3	5 5	m m	84 69	C C	13 13
	3.		$^3P-^1S$	1213.0 1366.5	9302 18561	91743 91743	3 5	1 1	m e	1150 4.9	C D	13 13
	4.		$^1D-^1S$	2288.9	48068	91743	5	1	e	9.2	D	13
[Fe XIV]	1.	$3p-3p$	$^2P^{\circ}-^2P^{\circ}$ (1F)	5303.4	0	18853	2	4	m	60.3	B	2,14
[Fe XV]	1.	$3s^2-3s3p$	$^1S-^3P^{\circ}$	394	0	255687	1	5	mq	1.8	DE	17
	2.	$3s3p-3s3p$	$^3P^{\circ}-^3P^{\circ}$ (1F)	7058.6	241531	255687	3	5	m	37.7	C	14

Cobalt

[Co XII]

Ground State

 $1s^2 2s^2 2p^6 3s^2 3p^4 3P_2$

Ionization Potential

 $[2710000] \text{ cm}^{-1} = [336] \text{ eV}$

For the spectrum of [Co XII], calculations by Krueger and Czyzak [13] are available and have been used for this tabulation. The calculations are based on self-consistent field wave functions and include the spin-

orbit and spin-spin and spin-other-orbit interactions; experimental values for the energy intervals are used whenever available.

[Co XII]

No.	Transition array	Multiplet	$\lambda(\text{\AA})$	$E_i(\text{cm}^{-1})$	$E_k(\text{cm}^{-1})$	g_i	g_k	Type of transition	$A_{ki}(\text{s}^{-1})$	Accuracy	Source
1.	$3p^4-3p^4$	$^3P-^3P$	6305	0	15856	5	3	m	84	C	13
2.		$^3P-^1D$	3801	15856	42158	3	5	m	12.7	C	13

Nickel

[Ni I]

Ground State

 $1s^2 2s^2 2p^6 3s^2 3p^6 3d^8 4s^2 3F_4$

Ionization Potential

 $61579 \text{ cm}^{-1} = 7.635 \text{ eV}$

List of tabulated lines

Wavelength [Å]	No.*	Wavelength [Å]	No.*
4523.16	4	7393.71	1
4565.6	8	7395.79	3
4710.8	8	7464.39	3
4813.27	4	7507.44	5
5027.34	4	7908.30	5
5348.4	12	7929.70	11
6404.46	3	7990.1	2
6437.70	7	8111.97	11
6489.61	7	8194.57	11
6604.30	7	8201.77	1
6730.25	7	8466.38	5
6787.00	7	8832.31	10
6941.63	3	8843.42	1
7002.02	3	9887.18	9
7130.24	7	11650	14
7193.97	7	15400	15
7218.8	6	45180	13
7243.99	3	47860	13

*The numbers in the lists of tabulated lines refer to the running multiplet numbers of the tables. ("Lists of tabulated lines" have been given for all spectra where 20 or more lines have been tabulated.)

The values for [Ni I] are taken from a 1964 calculation by Garstang [3]; this calculation includes limited configuration interaction arising from the three lowest configurations $3d^{10}$, $3d^94s$, and $3d^84s^2$. The tabulated data are estimated to be accurate within a factor of two, with the electric quadrupole values probably not quite as accurate as the magnetic dipole transition probabilities, since the radial integrals had to be obtained by extrapolation of results for various stages of ionization of Mn, Fe, and Ni, which had been derived in earlier work (see also ref. [3]).

[Ni I]

No.	Multiplet	$\lambda(\text{\AA})$	$E_i(\text{cm}^{-1})$	$E_k(\text{cm}^{-1})$	g_i	g_k	Type of transition	$A_{ki}(\text{s}^{-1})$
1.	a^3F-b^1D (1F)	7393.71 8201.77 8843.42	0 1332 2217	13521 13521 13521	9 7 5	5 5 5	e m e m e	0.0056 0.39 7.6(-4)* 0.17 2.0(-4)}
2.	a^3F-a^1S	7990.1	2217	14729	5	1	e	1.8(-4)
3.	a^3F-a^3P (2F)	6404.46 6941.63 7243.99 7002.02 7395.79 7464.39	0 1332 2217 1332 2217 2217	15610 15734 16017 15610 15734 15610	9 7 5 7 5 5	5 3 1 5 3 5	e e e m m m	0.032 0.025 0.031 0.15 0.0056 0.0022
4.	a^3F-a^1G (3F)	4523.16 4813.27 5027.34	0 1332 2217	22102 22102 22102	9 7 5	9 9 9	m e m e e	0.32 2.2(-4) 0.16 3.8(-6) 3.0(-4)
5.	a^3D-b^1D (4F)	7507.44 7908.30 8466.38	205 880 1713	13521 13521 13521	7 5 3	5 5 5	e e e	0.014 0.017 4.5(-4)
6.	a^3D-a^1S	7218.8	880	14729	5	1	e	0.068
7.	a^3D-a^3P (5F)	6489.61 6730.25 6437.70 6604.30 6787.00	205 880 205 880 880	15610 15734 15734 16017 15610	7 5 7 5 5	5 3 3 1 5	e e e e e	0.074 0.012 0.092 0.19 0.018

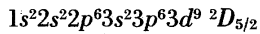
[Ni I]—Continued

No.	Multiplet	$\lambda(\text{\AA})$	$E_i(\text{cm}^{-1})$	$E_k(\text{cm}^{-1})$	g_i	g_k	Type of transition	$A_{ki}(\text{s}^{-1})$
		7130.24	1713	15734	3	3	e	0.053
		7193.97	1713	15610	3	5	e	0.0093
8.	a^3D-a^1G	4565.6	205	22102	7	9	e	7.9(-4)*
		4710.8	880	22102	5	9	e	0.080
9.	a^1D-b^1D (6F)	9887.18	3410	13521	5	5	e	0.012
10.	a^1D-a^1S (7F)	8832.31	3410	14729	5	1	e	0.31
11.	a^1D-a^3P (8F)	8194.57	3410	15610	5	5	e	0.024
		8111.97	3410	15734	5	3	e	4.7(-4)
		7929.70	3410	16017	5	1	e	1.1(-5)
12.	a^1D-a^1G	5348.4	3410	22102	5	9	e	0.44
13.	b^1D-a^3P	47860	13521	15610	5	5	m	0.072
		45180	13521	15734	5	3	m	0.063
14.	b^1D-a^1G	11650	13521	22102	5	9	e	4.1(-4)
15.	a^3P-a^1C	15400	15610	22102	5	9	e	4.3(-5)

*The number in parentheses following the tabulated value indicates the power of ten by which this value has to be multiplied.

[Ni II]

Ground State



Ionization Potential

$$146541.56 \text{ cm}^{-1} = 18.168 \text{ eV}$$

List of tabulated lines

Wavelength [Å]	No.*						
3074.11	5	4294.70	3	5711.46	13	7102.84	12
3076.1	5	4310.46	9	6007.34	7	7256.16	6
3223.2	5	4314.92	9	6365.52	7	7307.82	6
3378.55	4	4326.85	2	6441.1	12	7379.57	1
3439.29	4	4461.54	9	6467.52	7	7413.33	1
3559.86	4	4485.87	2	6668.16	1	7612.96	6
3627.35	4	4628.77	2	6700.61	7	7694.82	6
3993.65	3	5064.5	8	6791.61	7	8033.86	6
4025.80	3	5132.8	8	6794.37	6	8303.23	1
4033.56	3	5269.16	13	6813.73	7	8704.24	11
4143.17	9	5274.27	8	6848.8	12	9957.23	11
4147.30	9	5275.83	13	6911.05	6	10209.1	11
4201.74	2	5281.46	8	6956.25	7	10459.8	10
4249.48	3	5431.39	8	7054.37	7	11359.9	10
4285.90	3	5703.64	13	7078.25	7	12323.3	10

*The numbers in the lists of tabulated lines refer to the running multiplet numbers of the tables. ("Lists of tabulated lines" have been given for all spectra where 20 or more lines have been tabulated.)

The data in this compilation are taken from calculations by Garstang [7]. His work includes limited configuration interaction which Garstang finds to be a substantial effect for transitions between the $3d^84s$ and $3d^9$ configurations, but not for transitions within the

$3d^84s$ configurations. The tabulated data are estimated to be accurate within a factor of two. For a detailed discussion of the assessment of the accuracy of forbidden transition probabilities, we refer to the General Introduction.

[Ni II]

No.	Multiplet	$\lambda(\text{\AA})$	$E_i(\text{cm}^{-1})$	$E_k(\text{cm}^{-1})$	g_i	g_k	Type of transition	$A_{ki}(\text{s}^{-1})$
1.	a^2D-a^2F (2F)	7379.57	0	13550	6	8	e	0.14
		7413.33	1507	14997	4	6	e	0.11
		6668.16	0	14997	6	6	e	0.062
		8303.23	1507	13550	4	8	e	0.0076
2.	a^2D-b^2D (3F)	{ 4326.85	0	23108	6	6	m	1.2 }
		{ 4485.87	1507	23796	4	4	e	0.24 }
		{ 4201.74	0	23796	6	4	m	0.098 }
		{ 4628.77	1507	23108	4	6	e	0.51 }
3.	a^2D-a^4P (4F)	{ 3993.65	0	25036	6	6	m	0.040 }
		{ 4294.70	1507	24788	4	4	e	0.049 }
		{ 4033.56	0	24788	6	4	m	0.034 }
		{ 4285.90	1507	24836	4	2	e	0.043 }
		{ 4249.48	1507	25036	4	6	m	1.9(-4)* }
		{ 4025.80	0	24836	6	2	e	0.0076 }
		{ 3559.86	1507	29593	4	2	m	0.14 }
		{ 3378.55	0	29593	6	2	e	0.0022 }
4.	a^2D-a^2P (5F)	{ 3627.35	1507	29071	4	4	m	3.7 }
		{ 3074.11	0	29071	6	4	e	3.0 }
		{ 3076.1	0	32499	6	10	e	0.023 }
		{ 3223.2	1507	32523	4	8	e	1.1 }
5.	a^2D-a^2G (6F)	{ 7256.16	9331	23796	8	4	e	0.29 }
		{ 7307.82	9331	23108	8	6	m	4.0 }
		{ 7694.82	10116	23796	6	4	e	3.0 }
		{ 7612.96	10664	23108	4	6	m	0.0042 }
6.	a^4F-b^2D (7F)	{ 8033.86	10664	23796	6	4	e	0.019 }
		{ 6794.37	8394	23108	10	6	e	0.0058 }
		{ 6911.05	9331	23796	8	4	e	0.17 }
		{ 7256.16	9331	23108	8	6	m	0.0042 }
		{ 7307.82	10116	23796	6	4	e	0.39 }
		{ 7694.82	10116	23108	6	6	m	0.0023 }
		{ 7612.96	10664	23796	4	4	m	0.012 }
		{ 8033.86	10664	23108	4	6	m	0.019 }
		{ 6791.61	10116	24836	6	2	e	0.0095 }
		{ 6365.52	9331	25036	8	6	m	0.020 }
7.	a^4F-a^4P (8F)	{ 6013.73	10116	24788	6	4	e	0.21 }
		{ 7054.37	10664	24836	4	2	e	0.0070 }
		{ 6700.61	10116	25036	6	6	m	0.12 }
		{ 7078.25	10664	24788	4	4	e	0.014 }
		{ 6956.25	10664	24836	4	6	m	0.025 }
		{ 6467.52	9331	24788	8	4	e	0.0082 }
		{ 6007.34	8394	25036	10	6	e	0.024 }
		{ 6791.61	10116	24836	6	2	e	0.0011 }

[Ni II]

No.	Multiplet	$\lambda(\text{\AA})$	$E_i(\text{cm}^{-1})$	$E_k(\text{cm}^{-1})$	g_i	g_k	Type of transition	$A_{ki}(\text{s}^{-1})$
8.	a^4F-a^2P (9F)	5064.5	9331	29071	8	4	e	0.0019
		5132.8	10116	29593	6	2	e	0.0012
		5274.27	10116	29071	6	4	m	0.014
		{ 5281.46	10664	29593	4	2	m	0.0016
							e	1.8(-4)* }
		5431.39	10664	29071	4	4	m	0.0022
9.	a^4F-a^2G (10F)	4147.30	8394	32499	10	10	m	0.35
		4310.46	9331	32523	8	8	m	0.17
		4413.17	8394	32523	10	8	m	0.010
		4314.92	9331	32499	8	10	m	0.080
		4461.54	10116	32523	6	8	m	0.11
10.	a^2F-b^2D (11F)	10459.8	13550	23108	8	6	m	0.078
		11359.9	14996	23796	6	4	m	0.058
		12323.3	14996	23108	6	6	m	0.084
11.	a^2F-a^4P (12F)	8704.24	13550	25036	8	6	m	0.10
		10209.1	14996	24788	6	4	m	0.0096
		9957.23	14996	25036	6	6	m	0.070
12.	a^2F-a^2P (13F)	{ 7102.84	14996	29071	6	4	m	0.0092 }
		6441.1	13550	29071	8	4	e	0.053
		6848.8	14996	29593	6	2	e	0.047
13.	a^2F-a^2G (14F)	5275.83	13550	32499	8	10	m	0.087
		5708.64	14996	32523	6	8	m	0.044
		5269.16	13550	32523	8	8	m	0.13
		5711.46	14996	32499	6	10	e	2.3(-4)

*The number in parentheses following the tabulated value indicates the power of ten by which this value has to be multiplied.

[Ni III]

Ground State

Ionization Potential

$$1s^2 2s^2 2p^6 3s^2 3p^6 3d^8 \ 3F_4$$

$$283700 \text{ cm}^{-1} = 35.17 \text{ eV}$$

The data in this compilation are taken from calculations by Garstang [7]. The transitions occur between the levels of the $3d^8$ configuration, which is well separated from the $3d^74s$ configuration; thus, any interaction effects have been neglected in the calculations. We

estimate that the data for the tabulated prominent lines are accurate within a factor of two. For a more detailed assessment of the accuracy of forbidden transition probabilities, we refer to the General Introduction.

[Ni III]

No.	Multiplet	$\lambda(\text{\AA})$	$E_i(\text{cm}^{-1})$	$E_k(\text{cm}^{-1})$	g_i	g_k	Type of transition	$A_{ki}(\text{s}^{-1})$
1.	a^3F-a^1D	7124.6	0	14032	9	5	e	0.0045
		{ 7889.9	1361	14032	7	5	m	0.48 }
		{ 8499.6	2270	14032	5	5	e	5.4(-4)* }
							m	0.21 }
2.	a^3F-a^3P	6000.0	0	16662	9	5	e	0.050
		6401.5	1361	16978	7	3	e	0.038
		6682.2	2270	17231	5	1	e	0.046
		{ 6533.7	1361	16662	7	5	m	0.11 }
		{ 6797.2	2270	16978	5	3	m	0.009 }
		{ 6946.4	2270	16662	5	5	e	0.0028 }
							m	0.013 }
							e	0.022 }
							e	7.2(-4) }

[Ni III]—Continued

No.	Multiplet	$\lambda(\text{\AA})$	$E_i(\text{cm}^{-1})$	$E_k(\text{cm}^{-1})$	g_i	g_k	Type of transition	$A_{ki}(\text{s}^{-1})$
3.	a^3F-a^1G	4326.1	0	23109	9	9	<i>m</i>	0.35
		4596.8	1361	23109	7	9	<i>m</i>	0.18
4.	a^1D-a^3P	38010	14032	16662	5	5	<i>m</i>	0.098
		33940	14032	16978	5	3	<i>m</i>	0.090

*The number in parentheses following the tabulated value indicates the power of ten by which this value has to be multiplied.

[Ni IV]

Ground State

 $1s^22s^22p^63s^23p^63d^7\ 4F_{9/2}$

Ionization Potential

[442800] $\text{cm}^{-1} = [54.90]\text{eV}$

The listed data are taken from a 1968 calculation by Garstang [8]. We have selected from this paper two multiplets for which tentative identifications of several lines have been established [54]. At the time of Garstang's calculations, no observational analysis of the [Ni IV] spectrum existed, so that no precise wavelengths for the forbidden lines were available. In the meantime, based on Garstang's predictions [8], Lambert and Thackeray [54] observed several lines of [Ni IV] in the spectrum of RR Telescopii. We have used their identifi-

cations for this compilation. We have, however, made no corrections in the transition probabilities on account of these new wavelengths since the changes are of the order of 1 percent or less. Because of the extrapolations involved in obtaining the wave functions, we estimate the uncertainties for this spectrum to be slightly higher than usual, but still within a factor of two. A more detailed discussion on the assessment of the accuracy of forbidden transition probabilities is presented in the General Introduction.

[Ni IV]

No.	Multiplet	$\lambda(\text{\AA})$	$E_i(\text{cm}^{-1})$	$E_k(\text{cm}^{-1})$	g_i	g_k	Type of transition	$A_{ki}(\text{s}^{-1})$
1.	a^4F-a^4P	5519.34	0	18113	10	6	<i>e</i>	0.062
		{ 5906.89	1188	18113	8	6	<i>m</i>	0.0047 }
		{ 6220.21	2041	18113	6	6	<i>e</i>	0.015 }
		{ 6452.21	2619	18113	4	6	<i>m</i>	0.0017 }
		{ 5822.30	1188	18359	8	4	<i>e</i>	6.1(-4)* }
		{ 6126.48	2041	18359	6	4	<i>m</i>	2.4(-4) }
		{ 6351.41	2619	18359	4	4	<i>m</i>	0.034
		{ 5912.06	2041	18951	6	2	<i>e</i>	0.0010 }
		{ 6121.27	2619	18951	4	2	<i>e</i>	0.019 }
		{ 5041.62	0	19829	10	10	<i>m</i>	9.0(-5) }
2.	a^4F-a^2G	5363.04	1188	19829	8	10	<i>m</i>	0.025
		4773.24	0	20944	10	8	<i>m</i>	0.032
		5060.38	1188	20944	8	8	<i>m</i>	0.32
		5288.59	2041	20944	6	8	<i>m</i>	0.24

*The number in parentheses following the tabulated value indicates the power of ten by which this value has to be multiplied.

[Ni XII]–[Ni XVI]

Ion	Ground state	Ionization potential
[Ni XII]	$1s^2 2s^2 2p^6 3s^2 3p^5 \ ^2P_{3/2}^o$	[2839000] cm ⁻¹ = [352.0] eV
[Ni XIII]	$1s^2 2s^2 2p^6 3s^2 3p^4 \ ^3P_2$	[3097000] cm ⁻¹ = [384.0] eV
[Ni XV]	$1s^2 2s^2 2p^6 3s^2 3p^2 \ ^3P_0$	[3742500] cm ⁻¹ = [464.00] eV
[Ni XVI]	$1s^2 2s^2 2p^6 3s^2 3p^2 \ ^2P_{1/2}^o$	[4025000] cm ⁻¹ = [499.0] eV

(a) For [Ni XII] and [Ni XVI], the line strength for the one magnetic dipole transition in the ground state configuration is a straight number which has been, for example, tabulated by Krueger and Czyzak [13] (listed also in the General Introduction of our previous transition probability compilation, NSRDS-NBS 22, table 4 [2]). The quantity presented here, the transition probability, should also be quite accurate, since the energy level difference required for the conversion from the line strength is accurately known from the wavelength observed in the solar corona.

(b) For [Ni XIII], the arithmetic averages of the values of Naqvi [15] and Malville and Berger [16] are presented. The two sets of data agree within a few percent and are identical for the first listed line. For Naqvi's line strength

data, we have applied newly observed wavelengths to convert them to the transition probabilities. For the data of Malville and Berger, on the other hand, we have taken the transition probabilities directly from their tables, since they do not present their line strength or wavelength data.

(c) No data could be listed for [Ni XIV]. Two lines of this spectrum have been recently identified in the solar corona (Jordan [49]), but no calculations for the transition probabilities are known.

(d) For the spectrum of [Ni XV], calculations by Krueger and Czyzak [13] are available and have been used for this tabulation. These calculations are based on self-consistent field wave functions and include the spin-orbit and spin-spin and spin-other-orbit interactions; experimental values for the energy intervals are used whenever available. For the case of the 3P_1 – 1D_2 transition, the tabulated value differs from the one originally presented by Krueger and Czyzak since we have substituted for the original wavelength a new, more accurate value.

(e) For some of the remaining higher stages of ionization of Ni, calculations of forbidden transition probabilities exist (see table 1 of the General Introduction). However, since no wavelengths have as yet been observed, we do not present any data.

[Ni XII–Ni XVI]

Ion	No.	Transition array	Multiplet	$\lambda(\text{\AA})$	$E_i(\text{cm}^{-1})$	$E_k(\text{cm}^{-1})$	g_i	g_k	Type of transition	$A_{ki}(\text{s}^{-1})$	Accuracy	Source
[Ni XII]	1.	$3p^5$ – $3p^5$	$^2P^o$ – $^2P^o$ (1F)	4231.2	0	23626	4	2	m	237	B	2, 13
[Ni XIII]	1.	$3p^4$ – $3p^4$	3P – 3P (1F)	5115.8	0	19541	5	3	m	156	C	15, 16
	2.		3P – 1D (2F)	2126.0	0	46984	5	5	m	236	C	15, 16
[Ni XV]	1.	$3p^2$ – $3p^2$	3P – 3P (1F)	8024.1 6701.7	14917 0	27376 14917	3 1	5 3	m m	22.1 56	C C	13 13
	2.		3P – 1D	2085.7	14917	62863	3	5	m	212	C	13
[Ni XVI]	1.	$3p$ – $3p$	$^2P^o$ – $^2P^o$ (1F)	3601.1	0	27762	2	4	m	192	B	2, 13